

A Thesis
On
**WEAR BEHAVIOR OF DUAL PARTICLE SIZE
(DPS) REINFORCED ALUMINUM ALLOY**

Submitted in the partial fulfillment of requirement for the degree of

Master of Technology

in

Material Science and Metallurgical Engineering

by

Suresh Kumar

(600902012)

Under the supervision of

Dr. O.P.Pandey

(Prof. & Head)

School of Physics and Materials science

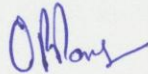


Thapar University, Patiala, (Punjab), INDIA

July-2011

Certificate

This is to certify that this thesis entitled “**Wear behavior of Dual particle size (DPS) zircon sand reinforced aluminum alloy**” which is being submitted by Mr. Suresh Kumar in fulfillment of the requirement for the award of degree of Master of Technology in school of physics and material science, Thapar university Patiala, (Punjab), India, is an exclusive record of candidate’s own research under our supervision. The thesis in part or in full has not been submitted in any other university or in institute for the award of any degree. The thesis is fit to be considered for the award of degree of Master of Technology.



Dr. O. P. Pandey

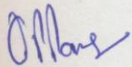
(Supervisor)

Prof. & Head

School of Physics & Material Science

Thapar University, Patiala, Punjab

Countersign By:

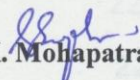


Dr. O.P. Pandey

Prof. & Head

School of Physics & Material Science

Thapar University, Patiala, Punjab



Dr. S. K. Mohapatra

Dean Academic Affairs

Thapar University, Patiala, Punjab

Contents	Pages
Acknowledgment	i
Abstract	ii
List of figure	iii
List of table	v
<u>Chapter-1: Introduction</u>	1-5
1 Introduction	1
1.1 Metal Matrix Composite (MMCs)	2
1.1.1 Types of MMCs	3
1.2 Fabrication methods of MMCs	4
References	5
<u>Chapter-2 : Literature Review</u>	6-16
<u>Chapter-3 Experimental and Characterization technique</u>	17-24
3.1 Fabrication Method of MMCs	17
3.1.1 Stir Casting	17
3.2 Experimental	19
3.3 Material Characterization	22
3.3.1 Microstructure analysis	22
3.3.2 Microhardness	22
3.3.3 Wear testing	23
References	24
<u>Chapter-4 :Result and discussion</u>	25- 60

4.1 Microstructural analysis	25
4.2 Line profile analysis	34
4.2.1 EDS Analysis	34
4.3 Hardness	35
4.4 Wear characteristics	36
4.4.1 Effect of sliding distance on wear rate	36
4.4.2 Effect of load on wear rate	40
4.4.3 Morphological analysis of worn surface and debris	44
4.5 EDS Analysis	58
Reference	59

Chapter-5: Conclusion and Future scope: **61-62**

5.1 Conclusion	61
5.2 Future work of the study	62

Acknowledgment

I am submitting my thesis report for the partial fulfillment of my M.Tech. degree. This work would not have been accomplished without the support, help and guidance of a large number of people. I express my deep gratitude and respect to my supervisor **Dr. O.P Pandey, Professor and Head, School of Physics and Material Science**, for his keen interest, strong motivation and constant encouragement during the course of the work. I thank him for his great patience, constructive criticism and myriad useful suggestions apart from invaluable guidance to me.

I would also like to thank **Dr. Kulvir Singh, Associate Professor, School of Physics and Materials Science** for his constant guidance and encouragement. I am also thankful to **Dr. Puneet Sharma, Dr. B. N. Chudasama, Dr. S.D. Tiwari** and all the faculty members of School of Physics and Materials Sciences for their constructive suggestions at different stages of this work.

It gives me immense pleasure to express my special thanks to **Mr. Ranvir Singh Panwar** (Ph.D. scholar), **Ms. Meenu** and **Mr. Vipin Sharma**, who always took keen interest in guiding me during my work.

I am extremely thankful to **Mr. Akshay Kumar, Mr. Gaurav Singla and Mr. Paramjyot Kumar Jha** in Thapar University, without whom the work would not have been possible.

I would like to convey my sincere gratitude to my friends and colleagues **Mr. Mukul Verma, Mr. Akshay Kumar, Mr. Pradeep Sirohi, Mr. Rajkumar, Mr. Abhishak Sharma and Ms. Richa Sharma** for their support and their timely help and valuable discussions. I owe my sincere thanks to all the staff members of School of Physics and Materials Science for their support and encouragement.

The meaning of my life and work is incomplete without paying regards to my respected parents whose blessings and continuous encouragement have shown me the path to achieve my goals. I would like to thank to my father **Shri Satyavir Singh**, my mother **Smt. Munni Devi** and my brothers (**Mr. N. Kumar and Mr. D. Kumar**) for their patience, moral support and constant co-operation whenever I was away from them.

And above all, I pay my regards to the **Almighty** for his love and blessings.



(Suresh Kumar)

Abstract

Present work aims to find the combined effect of coarse and fine size particle reinforcement of zircon sand in aluminum alloy LM13 on the wear behavior. Stir casting process was used to fabricate the composite. The composites are fabricated by varying the reinforcement of fine and coarse size zircon sand particles and compared with the single size reinforcement. Surface morphology was studied by using optical and Scanning electron microscope. Coarse and fine particle zircon sand of 106-125 μm and 20-32 μm size respectively are used in the present study. The wear test was carried out on pin-on disk machine. Microhardness measurement was done for developed composites. Wear track and debris are analyzed by SEM to study the wear mechanism. Line profile and EDS analysis is also done to validate the microstructural results. Study reveals that a combination of 3% and 12% coarse particle reinforced composite exhibits better wear resistance while 3% coarse and 12% fine particle reinforcement decreases the wear resistance. It is also observed that zircon sand particles provide effective nucleation site for the eutectic silicon. Microstructural examination shows globular and finely distributed eutectic silicon in the vicinity of the reinforced particles.

List of figures:

Fig 1: Optical micrograph of SPS 1 composites containing 15% fine particles showing (a) uniform particle distribution (b) micrograph showing dendritic and fragmented dendritic growth in particle depleted region (c) eutectic silicon exhibiting globular morphology around particles (d) SEM micrograph of SPS 1 composite showing uniform distribution of particles.

Fig2: Optical micrograph of SPS 2 composites containing 15% coarse particles (a) uniformly arranged particles in the alloy matrix (b) consistent and better bonding between zircon sand particle and alloy matrix and morphology of silicon at particle-matrix interface (c) long dendrite in particle depleted region and presence of silicon in between dendrite arm spacing (d) SEM micrograph of SPS 2 composite showing uniform distribution of fine particles with clustering at some places.

Fig.3: Optical micrograph of DPS 1 composites containing 12% coarse and 3% fine particles (a) coarse and fine particles are uniformly arranged in the alloy matrix (b) eutectic silicon morphology changes from acicular to globular in vicinity to particle (c) densely distributed globular silicon near the particle (d) SEM micrograph of DPS 1 composite showing distribution of fine and coarse particles.

Fig.4: Optical micrograph of DPS 2 composites containing 12% fine and 3% coarse particles (a) showing distribution of zircon sand particle (b) good bonding between zircon sand particle and alloy matrix (c) clustering of fine particles (d) SEM micrograph of DPS 2 composite showing the particle distribution and porosity.

Fig.5: SEM micrograph of composites showing the homogeneous distribution of coarse and fine particles. (a) SPS 1(b) SPS 2 (c) DPS 1(d) DPS 2.

Fig. 6: Line profile analysis composite

Fig.7: EDS analysis of embedded Zircon sand particle in alloy matrix

Fig 8: Wear rate of composites against sliding distance at different loads (a) wear rate of SPS 1 LM13/ 15% Zircon sand fine particles [20-32 mm] (b) wear rate of SPS 2 LM13/ 15% Zircon sand fine particles [106- 125 mm] (c) Wear rate of DPS 1

LM13/ 15 % zircon sand[12%C +3%F] (d) Wear rate of DPS 2 LM13/ 15 % zircon sand [12%F +3%C].

Fig 9: Bar graphical presentation of Wear rate at different loads (a) wear rate comparison of SPS 1 and SPS 2 (b) wear rate comparison of SPS 1 and DPS 2 (c) wear rate comparison of SPS 2 and DPS 1 (d) wear rate comparison of SPS 1, SPS 2, DPS 1 and DPS 2.

Fig 10: Wear rate of composites at different loads

Fig.11: SEM micrograph of worn out surface of SPS 1 composite at different loads (a) 1kg (b) 2kg (c) higher magnification at 2kg (d) 3kg (e) 4kg (f) 5kg.

Fig.12: SEM micrograph of Wear debris generated of SPS 1 at (a) 3kg (b) 4kg (c) 5kg

Fig.13: SEM micrograph of worn out pin surface of SPS 2 composite at different loads (a) 1kg (b) 2kg (c) 3kg (d) 4kg (e) 5kg (f) higher magnification at 5 kg

Fig.14. SEM micrograph of Wear debris generated of SPS 2 at (a) 1 kg (b) 3kg (c) 4kg (d) 5kg

Fig.15: SEM micrograph of Wear debris generated of SPS 2 at (a) 1 kg (b) 3kg (c) 4kg (d) 5kg Fig.14: SEM micrograph of worn out pin surface of DPS 1 composite at different loads (a) 1kg (b) 2kg (c) 3kg (d) 4kg (e) 5kg (f) lower magnification at 5 kg

Fig.16: SEM micrograph of Wear debris generated of DPS 1 at (a) 4kg (b) 5kg (c) 3kg

Fig.17: SEM micrograph of worn out pin surface of DPS 2 composite at different loads (a) 1kg (b) 2kg (c) 3kg (d) 4kg (e) 5kg

Fig.18: SEM micrograph of Wear debris generated of DPS 2 at (a) 1kg (b) 1kg (c) 2kg (d) 3kg (e) 4kg (f) 5kg

Fig.19: EDS analysis of composite wear debris

List of tables:

Table 1: Composition of the LM13 alloy in wt %

Table 2: Reinforcement combination of DPS composites

Table 3: Chemical composition of Keller' reagent

CHAPTER-1

Introduction

1. Introduction:

Aluminum alloy matrix with ceramic particles as a reinforcement is of great interest due to flexibility of tailoring the desired properties needed in engineering applications [1]. Some of the aluminum alloys exhibit wide range of properties but lack in tribological properties, which limits its use to certain applications [2]. Fabrication of aluminum matrix composite with reinforcement of hard particles is the widely used option for enhancing tribological properties as compared to other techniques, in terms of ease and economics involved along with achievement of desired properties [3].

Aluminum and its alloys with hard ceramic particles particulates reinforcement impart a combination of properties which are not achievable in either of the constituents individually. Aluminum alloys provide a good matrix for the development of particulate reinforced composites owing to their low density, high specific strength, high corrosion resistance, ease of fabrication and low cost. Zircon sand ($ZrSiO_4$) particles have a high modulus, high hardness and excellent thermal stability which when reinforced with Al-alloys make them highly attractive materials. Under suitable processing condition properties can be tailored to meet the diverse demands of various engineering applications [4].

In recent years many processing techniques have been developed to prepare particulate reinforced metal matrix composites. These techniques are stir casting, liquid metal infiltration, squeeze casting, spray co-deposition, powder metallurgy etc. Among the variety of processing techniques available for particulate or discontinuous reinforced metal

matrix composites, stir casting is one of the methods accepted for the production of large quantity composites. It is attractive because of simplicity, flexibility and most economical for large sized components to be fabricated [1-5].

In recent years numerous research works have been reported on production of MMCs by stir casting technique, but very limited research work has been done on dual size particle and no work has been reported on wear behavior of aluminum composites reinforced with dual size zircon particles.

Therefore, the present study is aimed to analyze the combined effect of both coarse and fine size particle reinforcement in aluminum alloy composite. Study mainly focused on investigating the microstructure and mechanical properties of dual particle size zircon sand reinforced LM13 alloy. The effects of dual size particles on the mechanical properties, microstructures and wear resistance of the particulate reinforced composite at room temperature have been analyzed.

1.1 Metal matrix composites (MMCs):

Metal matrix composites (MMCs), like all composites; consist of at least two chemically and physically distinct phases, suitably distributed to provide properties not obtainable with either of the individual phases. Generally, there are two phases, e.g., a fibrous or particulate phase, distributed in a metallic matrix. Examples SiC particle reinforced Al matrix composites used in aerospace, automotive, and thermal management applications.

With respect to metals, MMCs offer the following advantages:

- Major weight savings due to higher strength-to-weight ratio with exceptional dimensional stability (compare, for example, SiC,/Al to Al).
- Higher elevated temperature stability, i.e., creep resistance,
- Significantly improved cyclic fatigue characteristics.

With respect to PMCs (Polymer matrix composite), MMCs offer these distinct advantages:

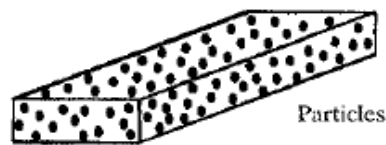
- Higher strength and stiffness,
- Higher service temperatures,
- Higher electrical conductivity (grounding, space charging),

- Higher thermal conductivity,
- Better transverse properties.

1.1.1 Types of MMCs:

All metal matrix composites have a metal or a metallic alloy as the matrix. The reinforcement can be metallic or ceramic. In general, there are three kinds of metal matrix composites (MMCs):

- (i) Particle reinforced MMCs.
- (ii) Short fiber or whisker reinforced MMCs.
- (iii) Continuous fiber or sheet reinforced MMCs.



Different types of metal matrix composites.

Particle reinforced MMCs:

Particle or discontinuously reinforced MMCs (the term discontinuously reinforced MMCs is commonly used to indicate metal matrix composites having reinforcements in the form of short fibers, whiskers, or particles) have assumed special importance for the following reasons:

- Short fiber or whisker Continuous fiber Particle reinforced composites are inexpensive vis-a-vis continuous fiber reinforced composites.
- Conventional metallurgical processing techniques such as casting or powder metallurgy, followed by conventional secondary processing by rolling, forging, and extrusion can be used.
- Higher use temperatures than the unreinforced metal.
- Enhanced modulus and strength.
- Increased thermal stability.
- Better wear resistance.
- Relatively isotropic properties compared to fiber reinforced composites.

1. 2 Methods of fabrication of MMCs:

- Stir casting.
- Spray casting.
- Powder Metallurgy.
- In-Situ fabrication techniques.
- Solid State methods.

References cited in this chapter:

- [1] J. Hashim, L. Looney and M.S.J. Hashmi, Metal matrix composites: production by the stir casting method, *Journal of Materials Processing Technology* 92-93 (1999) 1-7
- [2] Sanjeev Das, Siddhartha Das, Karabi Das, Abrasive wear of zircon sand and alumina reinforced Al-4.5 wt% Cu alloy matrix composites – A comparative study, *Composites Science and Technology* 67 (2007) 746–751.
- [3] S. Das, D.P. Mondal and G. Dixit, Correlation of Abrasive Wear with Microstructure and Mechanical Properties of pressure Die-Cast Aluminum Hard-Particle Composite, *Metallurgical and Materials Transactions A*, Volume 32a, March 2001—633-642
- [4] R. Sagar and R. Purohit, Fabrication and testing of Al-SiCp composite valve seat inserts, *Int. J. Adv. Manuf. Technol.* (2006) 29: 922–928
- [5] J. Hashim, The Production of Cast Metal Matrix Composite by a Modified Stir Casting Method, *Jurnal Teknologi*, 35(A) Dis. 2001: 9–20

CHAPTER-2

Litrature Review

Rajan et al. [1] in 1998 have proposed that there are different types of coatings known as metallic, ceramic, by layer, multilayer's etc. Metallic coatings improve the wettability of the reinforcement and prevent the excessive interfacial reaction by enrichment of the coated metal in the matrix near to the interface. A ceramic coating reduces the interfacial reaction by acting as a diffusion barrier between the reinforcement and the matrix. Most of the ceramic coating techniques are expensive. Multilayer coating leads to the multifunctional behavior of the coatings such as wetting agent, diffusion and reaction barriers and releaser of thermal residual stress.

Hashim et al. [2] in 1999 have proposed that processing variables such as holding temperature, stirring speed, size of the impeller, and the position of the impeller in the melt are among the important factors to be considered in an impact on mechanical properties. These are determined for the production of cast metal matrix composites as these have by the reinforcement content, its distribution, the level of the intimate contact of the wetting with the matrix materials, and also the porosity content. Therefore, by controlling the processing conditions as well as the relative amount of the reinforcement material, it is possible to obtain a composite with a broad range of mechanical properties. The method is potentially very cost effective, but widespread adoption is dependent on a satisfactory resolution of the technical difficulties presented.

Maruyama et al. [3] in 1999 have proposed that there are now a number of important production applications for discontinuous reinforcement aluminium, which span the

transportation, aerospace, recreation, and electronics industries and that demonstrate the material's attractive combination of structural, thermal management, and wear properties. While large materials suppliers have mostly exited the area, many smaller suppliers are forging ahead to make a success discontinuous reinforcement aluminium. Expanding this success depends upon the ability of researchers and engineers to continue increasing our fundamental understanding of the materials.

Gui et al. [4] in 2002 have proposed that the vacuum stir casting process is developed to produce SiC particle-reinforced Mg-Al9Zn and Mg-Zn5Zr cast magnesium matrix composites. No macro segregation of SiC particles and gas bubbles can be found in the composite ingots. This process can eliminate the entrapment of external gas onto melt and oxidation of magnesium during stirring synthesis. In the Mg-Zn5Zr/15SiCp composite, some agglomerations of SiC particles can be seen. At the same stirring process conditions, the wettability of SiC by magnesium in the Mg-Zn5Zr melt is worse than that in the Mg-Al9Zn melt. Both composites exhibit significant improvement in yield strength and elastic modulus, especially for the Mg-Al9Zn/ 15SiCp composite. A 112% increase in yield strength and 33% increase in elastic modulus are obtained for this composite compared with the unreinforced magnesium alloy, while increases of 24 and 21%, respectively, were observed for the Mg-Zn5Zr/15SiCp composite.

Surappa et al. [5] in 2003 indicates that several challenges must be overcome in order to intensify the engineering usage of AMCs. Design, research and product development efforts and business development skills are required to overcome these challenges. In this pursuit there is an imperative need to address the following issues. Science of primary processing of AMCs need to be understood more thoroughly, especially factors affecting the microstructural integrity including agglomerates in AMCs. There is need to improve the damage tolerant properties particularly fracture toughness and ductility in AMCs. Work should be done to produce high quality and low cost reinforcements from industrial wastes and by-products. Efforts should be made on the development of AMCs based on non-standard aluminium alloys as matrices. There is a greater need to classify different grades of AMCs based on property profile and manufacturing cost. There is an urgent need to

develop simple, economical and portable non-destructive kits to quantify undesirable defects in AMCs.

Chaudhary et al. [6] in 2004 were proposed that 11 wt% of TiO_2 could be successfully incorporated into the Al-2Mg melt by vortex method. Greater degree of segregation of TiO_2 has been observed at the top and bottom of castings. Micro voids are observed in the particles enriched zone. A phase transformation has been observed during the resistivity and DSC measurements owing to the precipitation of TiAl_3 phase. Cold and hot rolling of the composite is successfully carried out to 40% and 50% reduction, respectively. Hardness of the composite is greater than the base alloy, which can be attributed to the presence of higher dislocation density in the matrix due to the difference in thermal properties between the matrix and dispersoids. The improved tensile behavior of cold rolled composite aged at 400°C could be due to the precipitation of the Al_3Ti phase.

Prabu et al. [7] in 2005 have concluded from the microstructure analysis that during lower speed and lower stir time particle clustering occurred in some places, and some places were identified without SiC inclusion. By increasing the stirring speed and stirring time better homogeneous distribution of SiC in the Al matrix were found. Better distributions of SiC were found at 600 rpm and 10min stirring time condition. It was found from the hardness test that the speed and time influence the hardness of the composite. Higher stirring speed and stirring time, gives better hardness composite of MMC as compared to as-cast condition. Better hardness composite was obtained from 600 rpm and 10min stirring time processing condition.

Nikanorov et al. [8] in 2005 have synthesized Al-Si alloy and concluded that Al-Si alloys prepared by rapid cooling of levitated melts were used to elucidate the effect of Si content on mechanical properties. The structure and mechanical properties of quenched Al-Si alloys in a wide compositional range from 11.5 up to 35wt% Si were investigated. Extreme condition for silicon concentration were found for the average temperature coefficient of Young's modulus for cooling from 500 to 20°C , the hysteresis of Young's modulus for heating and cooling over this range, and the yield point. These extreme correspond to

solidification in the region yielding coupled eutectic-like growth. In this region the process of Guinier–Preston zones creation is hampered. It explains extreme of concentration dependences of temperature coefficients and temperature hysteresis of Young’s modulus. The decrease of yield point for lower Si concentrations is attributed not only to the decreasing size and concentration of Si in the eutectic structure, but also to an increased number of plastic dendrites of solid solution. The decrease of the yield point of hypereutectic alloys with increasing the Si content is attributed to the increase of the interfacial area between primary Si crystals and eutectic matrix.

Jian-min et al. [9] in 2006 have explained the mainly four kinds of defects in SiCp/A356 composites if an unsuitable stir casting process is used. Black inclusions are SiC agglomerates, silver spots are Al-Fe-Si phase particles, white inclusions are SiC particles adhering to Al₂O₃ and the pores are caused by gas bubbles and agglomerated SiC particles. An improved stir casting process is established for fabricating SiCp/A356 composites with good mechanical properties and less defects.

Das et al. [10] in 2006 have concluded that wear resistance properties of Al–4.5 wt% Cu alloy improves significantly after addition of alumina and zircon particles. Decrease in particle size improves wear resistance property for both alumina and zircon reinforced composites as smaller particle reinforced composite has higher hardness and is more efficient in blunting SiC [15] abrading surface. Zircon reinforced composite shows better wear resistance than alumina reinforced composite due to its superior particle–matrix bonding.

Basavarajappa et al. [11] in 2007 have evaluated that the addition of SiCp reinforcement to Al 2219 alloy increases the wear resistance of the composites. The addition of graphite reinforcement in Al–SiCp composites further increases the wear resistance at all sliding speeds and effectively avoids the occurrence of severe wear. The subsurface deformation from the contact surface to the region where the bulk hardness of the composite is reached can be divided into three zones. Zone 1 extends up to a depth of 60µm from the worn surface for both Al 2219/15SiCp and Al 2219/15SiCp-3Gr composite. Zone 2 corresponds

to the subsurface that is 60–180 μm from the worn surface in Al 2219/15SiCp and 60–140 μm from the worn surface in Al 2219/15SiCp-3 graphite composite. Zone 3 is the region that remains unaltered. Variation of microhardness and the depth of deformation in the subsurface regions in Al 2219/15SiCp composite are different for different sliding speeds. The microhardness just below the wear surface is very high and as the depth increases the microhardness decreases. In the severe wear region the initial microhardness just below the worn surface is less, which can be attributed to the material removal in the form of sheets and particle pull out, exposing un-deformed material.

Grosz et al. [12] in 2007 in their work have shown that ceramic particles in the form of silicon carbide and amorphous glassy carbon have an influence on both temperature change and the time of aluminum castings solidification. They also have influence on the structure and particles displacement of the casts. The changes results, first of all, from disparate physical properties of the particles used (thermal conductivity, mass density). The presented research results represent a preliminary study. The on-going research refers to the influence of the type, size and volume fraction of reinforcing particles on solidification and crystallization of heterophase composites.

Purohit et al. [13] in 2007 have given an overview of the present and future applications of magnesium matrix composites have been presented. Basically magnesium based metal matrix composites (MMCs) have attracted considerable interest because of their attractive mechanical properties over monolithic alloy. However, several drawbacks (most amenable to technical or institutional fixes) have limited the growth of Mg usage in automobiles. On the other hand, in aerospace industry high cost can be justified, high-performance materials and processes, several new materials like Mg-MMC have been evaluated. The most important factors are the material's physical properties, some of which are less desirable than its low density. Major limitations of magnesium-based materials include low ductility and low resistance to fracture. It has been shown convincingly that use of particulates in nano length scales in pure magnesium can circumvent these limitations. Studies have shown that the use of nano-sized reinforcements imparts an excellent combination of strength and ductility Mg is very reactive, but it can be protected with

applied coatings or simply allowed to build up a naturally occurring oxide or sulfate coating. Corrosion has also been a concern. However, development of new alloys has helped achieve acceptable properties. The key factor that inhibits the massive use of Mg is its relatively high and unstable price. However, this may be compensated by the lower fabrication and joining costs of magnesium. Substitution of presently used materials for aerospace and automotive components and body structures by lightweight magnesium matrix composites would enable secondary weight savings, and lifetime fuel costs are reduced, so the total life-cycle cost of a Mg-MMC part may actually be lower than that of one made from another material.

Aigbodion et al. [14] in 2007 have synthesized Al-Si-Fe alloy with silicon carbide addition using double stirring casting method and concluded that addition of silicon carbide particles using this method to Al-Si-Fe alloy increases both the yield strength, ultimate tensile strength and hardness values up to a maximum values of 79.98, 106.12Nmm² and 67.0HRB, respectively, at 20% SiC addition. There is general slight increase in the apparent porosity of the composites with percentage SiC addition that is still lower than the recommended values. For optimum service performances of this alloy, silicon carbide addition should be between 15 and 20% and not exceed 20% in order to develop better necessary properties.

Abdizadeh et al. [15] in 2008 have proposed that the improvement of hardness and tensile strength of aluminum by incorporation of ZrSiO₄ and TiB₂ particles is due to the high strengthening and work-hardening at low strain in the composite system. This is caused by elastic properties of these ceramic particles that prevent plastic deformation of matrix metal. The best property values for Al-5% ZrSiO₄ are achieved at 750°C and for Al-5% TiB₂ at 950°C. This may be related to the lower heat expansion coefficient of TiB₂ than of ZrSiO₄ that induces a larger dislocation density at boundaries between matrix metal and TiB₂ particulates.

Jha et al. [16] in 2009 their works have described that numerous porosities present in the casting resulted in crack initiation. The crack propagated by interlinking of pores, and the

casting failed. The acicular Si eutectic facilitated the cracking by debonding from the matrix.

Zhang et al. [17] in 2010 have studied the effects of Ba modifier in aluminium alloy. It addition of 1.0 wt. % exhibited the best results for the mechanical properties of alloy. The modification caused the disappearance of primary silicon with the formation of solid solution dendrites and fine fiber or rod-like eutectic silicon instead of plate-like structures, resulting in a highly branched filamentary form with a better distribution of Si particles. The modification could also improve the wear resistance of the alloy. The Al–Mg–Si alloy with modification had good remelting property. The Al–Mg–Si alloy failed in a mixed-mode fracture comprised of intergranular fracture, quasi-cleavage plane, and transgranular shear.

Okafor et al. [18] in 2010 have evaluated the addition of $ZrSiO_4$ particles using Al-4.5%Cu alloy. It has led to an increase in both the strength and hardness and an overall reduction in toughness and density. Also, little increase in the apparent porosity of the composite with percentage increase in $ZrSiO_4$ addition was observed. From the result, maximum service performance of the Al-4.5Cu/ $ZrSiO_4$ particulate composite synthesis via squeeze casting should not exceed 15% in order to develop balance in the necessary properties. Pronounced increase in hardness value was observed by reinforcing the matrix alloy with 5-25% zircon sand. Al-4.5Cu/15% $ZrSiO_4$ particulate composite could be appreciable in automobile industries (brake drum, crankshafts, valves and suspension arms), recreational products (golf club shaft and head, skating shoe, bicycle frames and base ball shaft) and in construction company.

Amirkhanlou et al. [19] in 2010 have proposed that injection of milled (Al-SiCp)cp composite powder instead of untreated SiC particles into the melt decreases the SiC particle size, enhances the wettability between the molten matrix alloy and the reinforcements and improves the distribution of the reinforcement particles in the solidified matrix. Wettability and distribution of SiC particles are further improved by casting in semisolid state (compo casting) rather than in fully liquid state (stir casting).

Addition of SiC particles in the form of (Al-SiC)_p composite powder and casting in semisolid state increases the hardness of the composites by 10% and decreases the porosity by 68%. The impact energy is slightly influenced by the form of the reinforcement addition but the casting method does not influence the impact energy.

Jayaseelan et al. [20] in 2010 have proposed that stir casting specimen exhibited high hardness compared to powder metallurgy specimen. Stir casting specimens are finer grains in the microstructure than the powder metallurgy specimen. After extrusion both the extruded specimen exhibited reduced porosity, more uniform particle distribution, elimination of clusters and improved ductility and also both the specimens are experienced grain refinement and increased strength. The load required for extrusion was less for powder metallurgy process compared to stir casting process. From the above results it was concluded that stir casting specimens have higher strength compared to powder metallurgy specimen.

Suresha et al. [21] in 2010 have conducted the experiments on Al-SiC-Gr hybrid composite with combined reinforcement up to 10% Al-Gr and Al-SiC composites with reinforcement up to 10% using pin-on-disc equipment amount of reinforcement, sliding speed, load and sliding distance affect the wear of all the composites. Interactions exist among sliding speed, load and sliding distance in Al-SiC-Gr hybrid composites and between load and sliding distance in Al-Gr composites. Such interactions do not exist in Al-SiC composites. Increase of speed reduces wear by supporting mechanically mixed tribolayer and increase of load increases wear by reducing the role of tribolayer. Wear increases with sliding distance (due to unstable tribolayer) and it is the predominant factor affecting wear of all the composites.

Pradeep et al. [22] in 2011 have prepared the cast Al6063 - SiC composites were prepared successfully using liquid metallurgy techniques. Hardness of the composites was found to increase with increased SiC content. Finer the grain size better is the hardness and strength of composites leading to lowering of wear rates. The tensile strength of the composites was

found to increase with increased reinforcements in the composites. The percentage elongation of the composite material is found to be in decreasing trend with the increase in the percentage SiC content. The compressive strength of the composites also increased with increased reinforcements in the composites.

Behera et al. [23] in 2011 have recorded the solidification curves experimentally for Al alloy (LM6) and its composites with varied percentage of SiC particles from 7.5 wt% to 12.5 wt% in steps of 2.5 wt% and compared with the unreinforced matrix alloy .i.e. LM6. The introduction of SiCp in the matrix metal decreases the cooling rate, as the presence of SiCp in matrix metal increases. This is because of lower heat transfer rates during solidification owing to the reduction of thermal conductivity and effective thermal diffusivity of the composite system. The increase in weight percentage of SiCp in matrix metal decreases the rate of solidification rate. This indicates that the solidification rate is faster in case of unreinforced matrix alloy or containing low fraction of SiCp in the matrix. Addition of ceramic reinforcement to alloy enhances the eutectic solidification time, as the presence of insulating dispersoids i.e. SiCp plays a dominant role in reducing the cooling rates. The solidification time has also varied with the change in thickness of castings. The solidification time is less in case of thinner section in comparison with thicker section, due to rapid cooling of thinner section. This trend is similar to the monolithic metal and its alloys. Additions of Mg to the composite melt has multifunctional role. Apart from its well known function as a wetting promoter of ceramic particle with the aluminum alloy matrix, it leads to better contact at the metal/mould interface, thereby by enhancing the heat transfer rate. The forgeability test has been carried out at room temperature by upset method. The forgeability i.e. the percentage of deformation decreases on increasing the percentage of SiCp in the matrix metal and the middle part of the casting.

Reference cited in this chapter:

1. T .P.D. Rajan , R .M . Pillai, B.C .Pai, Journal of Material Science33(1998) 3491 - 3503
2. J. Hashim, L. Looney, and M. S. J.Hashmi. Journal of materials processing technology. 92-93: (1999) 1-7.
3. Benji Maruyama and Warren H. Hunt, JOM 51(1999)62-64
4. Manchang Gui, Jianmin Han, and Peiyong Li JMEPEG (2003) 12:128-134
5. M. K. Surappa, Aluminium matrix composites: Challenges and Opportunities. Sadhana Vol. 28, Parts 1 & 2, February/April 2003, pp. 319–334
6. S K Chaudhary, A K Singh, C S S Sivaramakrishana and S C Panigrahi Bull. Mater. Sci., Vol. 27, No. 6, December (2004) 517–521.
7. S. Balasivanandha Prabu , L. Karunamoorthy, S. Kathiresan, B. Mohan, Journal of Materials Processing Technology 171 (2006) 268–273
8. S.P. Nikanorov,M.P. Volkov, V.N. Gurin, Yu.A. Burenkov, L.I. Derkachenk ,B.K. Kardashev, L.L. Regel, W.R. Wilcox Materials Science and Engineering A 390 (2005) 63–69
9. Han Jian-min, Wu Zhao-ling, Cui Shi-haia, Li Wei-Jing and DuYong-ping Journal of Ceramic Processing Research. Vol. 8, No. 1 (2006) 74-77
10. Sanjeev Das, V. Udhayabanu, S. Das, K. Das, J. Mater Sci. (2006) 41:4668–4677
11. S. Basavarajappa, G. Chandramohan, Arjun Mahadevan, Mukundan Thangavelu, R. Subramanian, P. Gopalakrishnan Wear 262 (2007) 1007–1012
12. A.Dolata-Grosz, M. Dyzia, J.O Eleziona Archives of Materials Science and Engineering Volume 28Issue 7(2007)401-404
13. R. Purohit, A. Bharathi, A. Chandrashekar, M. Saxena, O. Gahlawat and P. Sharma INCCOM-6 Conference on Future Trends in Composite Materials and Processing
14. V.S. Aigbodion and S.B. Hassan, Material science and engineering A 447(2007) 355-360
15. H. Abdizadeha, H.R. Baharvandi, K. Shirvani Moghaddam, Materials Science and Engineering A 498 (2008) 53–58
16. Abhay K. Jha, K. Sreekumar Engineering Failure Analysis 16 (2009) 2433–2439

17. X.H. Zhang, G.C. Su, C.W. Ju, W.C. Wanga, W.L. Yan *Materials and Design* 31 (2010) 4408–4413
18. E. G. Okafor , V. S. Aigbodion, *Tribology in industry*, Volume 32, No. 2,(2010)31
19. S. Amirkhanlou, B. Niroumand. *Trans. Nonferrous Met. Soc. China* 20(2010) 788-793
20. V. Jayaseelan, K. Kalaichelvan, M. Kannan, S. Vijay Ananth *International Journal Of Applied Engineering Research* Volume 1, No1, 2010
21. S. Suresha, B.K. Sridhara *Composites Science and Technology* 70 (2010) 1652–1659
22. G.R.C. Pradeep, 2A. Ramesh, 3G.B. Veeresh Kumar Published in *International Journal of Advanced Engineering & Application*, Jan 2011 Issue
23. Rabindra Behera, A.Datta, D.Chatterjee, G.Sutradhar *International Journal of Scientific & Engineering Research*, Volume 2, Issue 1,(2011) 2229-5518

CHAPTER 3

Experimental and Characterization technique

3.1 Fabrication method of MMCs:

Liquid state fabrication of metal matrix composites involves incorporation of dispersed phase into a molten matrix metal, followed by its solidification. In order to provide high level of mechanical properties of the composite, good interfacial bonding (wetting) between the dispersed phase and the liquid matrix should be obtained. Wetting improvement may be achieved by coating the dispersed phase particles (fibers). Proper coating not only reduces interfacial energy, but also prevents chemical interaction between the dispersed phase and the matrix. The simplest and the most cost effective method of liquid state fabrication is Stir Casting.

3.1.1. Stir Casting:

Stir Casting is a liquid state method of composite materials fabrication, in which a dispersed phase (ceramic particles, short fibers) is mixed with a molten matrix metal by means of mechanical stirring. The liquid composite material is then cast by conventional casting methods and may also be processed by conventional Metal forming technologies. Metal matrix composites (MMCs) possess significantly improved properties including high specific strength specific modulus, damping capacity and good wear resistance compared to unreinforced alloys. There has been an increasing interest in composites containing low density and low cost reinforcements. Among various discontinuous dispersoids, now a days the particulate reinforced aluminum matrix composite are gaining importance because of their low cost with advantages like isotropic properties and the possibility of secondary processing facilitating fabrication of secondary components. The present investigation has

been focused on the utilization of abundantly available silicon in useful manner by dispersing it into aluminum to produce composites by stir casting method.

Conventional monolithic materials have limitations in achieving good combination of strength, stiffness, toughness and density. To overcome these shortcomings and to meet the ever increasing demand of modern day technology, composites are most promising materials of recent interest. Metal matrix composites (MMCs) possess significantly improved properties including high specific strength; specific modulus, damping capacity and good wear resistance compared to unreinforced alloys. Composites with silicon/Sic as reinforcement are likely to overcome the cost barrier for wide spread applications in automotive and small engine applications. It is therefore expected that the incorporation of silicon or sic particles in aluminum has the potential for conserving energy intensive aluminum and thereby, reducing the cost of aluminum products. Cast aluminum matrix particle reinforced composites have higher specific strength, specific modulus and good wear resistance as compared to unreinforced alloys. The particulate composite can be prepared by injecting the reinforcing particles into liquid matrix through liquid metallurgy route by casting. Casting route is preferred as it is less expensive and amenable to mass production. Among the entire liquid state production routes, stir casting is the simplest and cheapest one. The only problem associated with this process is the non uniform distribution of the particulate due to poor wettability and gravity regulated segregation. Mechanical properties of composites are affected by the size, shape and volume fraction of the reinforcement, matrix material and reaction at the interface. Among discontinuous metal matrix composites, stir casting is generally accepted as a particularly promising route, currently practiced commercially. Its advantages lie in its simplicity, flexibility and applicability to large quantity production. It is also attractive because, in principle, it allows a conventional metal processing route to be used, and hence minimizes the final cost of the product. This liquid metallurgy technique is the most economical of all the available routes for metal matrix composite production, and allows very large sized components to be fabricated. The cost of preparing composites material using a casting method is about one third to half that of competitive methods, and for high volume production, it is projected that the cost will fall to one-tenth. In general, the solidification synthesis of metal matrix composites involves producing a melt of the selected matrix material followed by the

introduction of a reinforcement material into the melt, obtaining a suitable dispersion. Metal matrix composite (MMC) is engineered combination of the metal (Matrix) and hard particle/ceramic (Reinforcement) to get tailored properties. Considerable research from all over the world has been devoted to metal matrix composite (MMC) research over the past few decades involving a broad area of MMC fabrication. In any type of the fabrication method used, wet ability and distribution of the reinforcement material in the alloy matrix are among the main problems. Many methods have been proposed to overcome this situation. However, ideas normally suitable for the preparation of materials and their use may not be suitable for different approaches.

In general stir casting of MMC involves producing a melt of selected matrix material followed by the introduction of reinforcement material into the melt and the dispersion of the reinforcing material through stirring. Stirring is carried out vigorously to form a vortex where the reinforcing particles are introduced through the side of the vortex. The formation of the vortex will drag not only the reinforcement particles into the melt, but also all impurities which are formed on the surface of the melt. The vortex will also entrap air into the mould which is extremely difficult to remove as the viscosity of the slurry increase.

3.2 Experimental:

In the present study well known piston alloy LM13 is used as matrix material and high purity zircon sand ($ZrSiO_4$) as reinforcement. LM13 alloy was obtained in the form of ingots. The compositional analysis of the alloy LM13 was done by wet chemical analysis which is shown in Table 1.

Table 1: Composition of the alloy LM13 in wt %

LM13 alloy	Si	Fe	Cu	Mn	Mg	Zn	Ti	Ni	Pb	Sn	Al
Wt. %	11.8	0.3	1.2	0.4	0.9	0.2	0.02	0.9	0.02	0.005	Balance

The synthesis of the composite was carried out by stir casting process. The detailed description of the process is similar to described in other work [1-4]. A weighted quantity of LM13 alloy were taken in a graphite crucible and melted in an electric furnace. The temperature was slowly raised to 850 °C. This molten metal was stirred using a graphite impeller at a speed 630 rpm to create the vortex. The impeller blades were designed in such way that it creates vortex to achieve the particle mixing. The vortex method is one of the better known approaches used to create and maintain a good distribution of the reinforcement material in the matrix alloy. The dual size zircon sand is mixed properly and preheated at a temperature of 450°C to drive off the moisture. After the formation of vortex in the melt, the sand particle was added with a spatula at the rate of 20–30 g/min. into the melt during stirring. The stirring was continued for another 5 min. even after the completion of particle feeding for homogeneous distribution of the sand particles. The mixture was poured in to the metal mould and solidified at room temperature conditions. During production of samples, the amount of charge materials, stirring duration and position of stirrer in the crucible were kept constant to minimize the contribution of variables related to stirring on distribution of second phase particles.

There are many factors which directly affect the properties of stir cast composite. So the factors such as stirrer geometry including blade angle, stirring time, stirring speed, pouring rate, temperature of melt etc. must be optimized to achieve better bunch of properties in the composite. To optimize uniform particle distribution into the melt, the stirring parameters were selected as stirring time of 12 minutes, 3 blade stirrer with a blade angle of 30° and stirrer immersion in liquid melt is at a position of two-third of the melt [3,4].

During fabrication of the DPS composite, zircon sand particle of two sizes were chosen for 15wt.% reinforcement. These were particles of size range 20-32 µm and 106-125µm. To compare and correlate the effect of particle size on mechanical and tribological properties, four different composites containing a total of 15wt% were fabricated, in which two composites were reinforced by dual size particle combined in the 4:1 ratio.

In the first combination of DPS (DPS1) there was 12 percent coarse and 3 percent fine zircon sand particles, whereas, in the second combination (DPS2) there was 3 percent

coarse and 12 per cent fine zircon sand particles. The two composites are synthesized by incorporation of only single size particle of fine (SPS1) and coarse particles (SPS2) of 15% by weight. The reinforcement combinations are represented in Table 2.

Table 2 Reinforcement combination of DPS composites

Composite	Fine (wt %) (20-32 μ m)	Coarse (wt %) (106-125 μ m)
SPS1	15	0
SPS2	0	15
DPS1	3	12
DPS2	12	3

Dry sliding wear tests of the reinforced and unreinforced alloys have been performed under the ambient temperatures between 25–30°C and relative humidity between 22–35%, using a pin-on-disc wear and friction monitor (Model TR-20, Ducom, Bangalore). The cylindrical shaped samples (30 x 8 mm) of composite were tested against the hardened EN32 steel disc having chemical composition (0.14% C, 0.52% Mn, 0.18% Si, 0.13% Ni, 0.05% Cr, 0.06% Mo, 0.019% P, 0.015% S, balance Fe) and hardness 65 HRC. Before testing, each specimen is cleaned with acetone.

3.3 Material characterization:

3.3.1. Microstructural analysis:

Composite (Al-Zr) samples were ground and mechanically polished for metallographic study. After polishing, these samples were etched with freshly prepared Keller's reagent. The surface morphology of each sample was studied with the help of optical microscope (Eclipse MA-100, Nikon) and scanning electron microscope (JOEL, JSM-6510LV). To study the presence of elements in the sample Energy-dispersive X-ray spectroscopy (oxford INCA) with model no. 51-ADD 0076 was used.

Table 3: Chemical composition of Keller' reagent

Composition	Dist. Water	HNO ₃	HCl	HF
Vol%	95ml	2.5ml	1.5ml	1ml

3.3.2. Microhardness:

The microhardness measurement at different phases of composites has been carried out to know the effect of reinforced particulates on the alloy matrix. Micro hardness of the LM13/Zircon sand composite was taken at 100 kgf load with vicker hardness testing machine (Mitutoyo with model no.MVK_HO) made in madras, India. Vicker hardness (H_v) was calculated by using the formula as

$$H_v = 1.854 \frac{F}{d^2} \text{ (approx.)}$$

Where F = load in Kgf, d = Arithmetic mean of the two diagonal, d_1 & d_2 in mm.

The average value of five indentations per sample has been taken. In order to check the binding nature of the particles, micro hardness was measured using diamond indenter of a load of 100 kgf on the surface of particle and interface as well as on matrix.

3.3.3. Wear testing

Wear test were conducted using polished pin samples with flat surfaces in the contact region but rounded in the corner and cleaned with acetone to remove dust or grease from the surfaces. Dry sliding wear tests were carried out against the counterface of a hardened and polished disk made of EN-31 steel having 65 HRC at a relative humidity of 36-56%. A study pin-on-disc machine supplied by Ducom, Bangalore (model TR20-CH400). The wear test pin samples have been prepared from composites and the diameters of the pins are 8mm. The test was conducted at the loads of 1 to 5 kg at the constant sliding velocity of 1.6m/s. However the wear characteristics have been noted down at room temperature.

The wear debris obtained after the 30 min of sliding of each test run were examined under SEM. The worn surfaces of the samples were also examined under SEM to know the wear mode of the worn surfaces.

References cited in this chapter:

1. M. K. Surappa, Aluminium matrix composites: Challenges and Opportunities, *Sadhana* Vol. 28, Parts 1 & 2, February/April 2003, pp. 319–334.
2. S. Amirkhanlou and B. Niroumand, Synthesis and characterization of 356-SiCp composites by stir casting and compocasting methods, *Trans. Nonferrous Met. Soc. China* 20(2010) 788-793.
3. J. Hashim, L. Looney and M.S.J. Hashmi, Particle distribution in cast metal matrix composites—Part I, *Journal of Materials Processing Technology* 123 (2002) 251–257.
4. J. Hashim, L. Looney and M.S.J. Hashmi, Particle distribution in cast metal matrix composites-Part II, *Journal of Materials Processing Technology* 12 (2002) 258–263

4.1 Microstructural analysis

The optical micrographs of reinforced composites are shown in Fig.1. The uniform and homogeneous distribution of reinforced particles has been observed in the optical micrographs of composites. The homogeneous distribution of the reinforcement phase is a prime requisite for a composite material to present its superior performance. Optical observation also shows that the dendritic growth is inhibited by the reinforced particles, which in turn provides better mechanical properties. The distribution of coarse particles with fine particles is in random fashion in the alloy matrix but they are uniformly arranged to serve their purpose. Optical micrograph of all composites shows smooth interface between particle and matrix, which indicates better bonding of zircon sand particles with LM13 matrix. A wide variation in matrix structure is observed due to the presence of zircon particulates of different size in the alloy matrix.

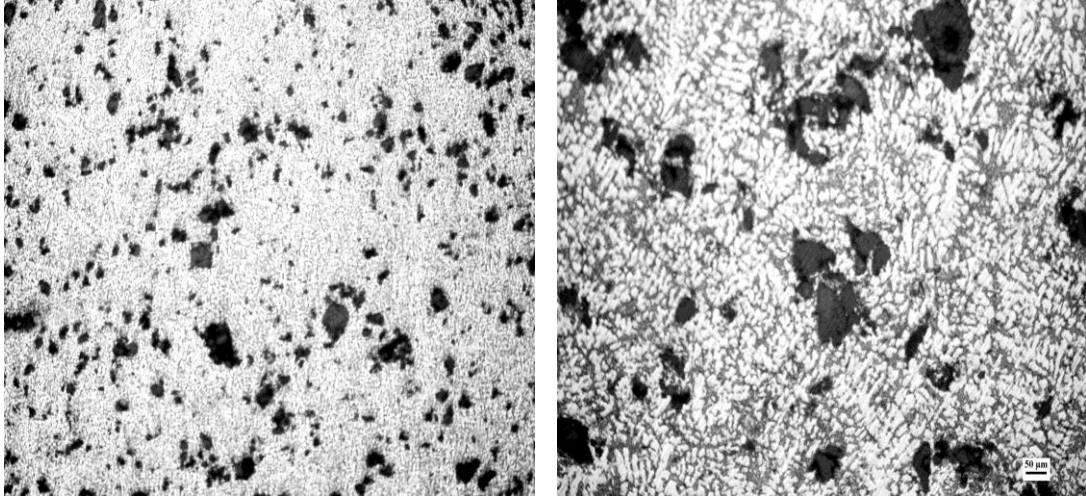
The optical micrograph of composites is captured at various magnification for investigating the particle bonding and distribution. The optical micrograph of SPS1 reinforced with 15% fine particles (20-32 μm) is shown in Fig.1. The Fig. 1(a) shows homogeneous distribution of reinforced particles in alloy matrix. Homogeneous distribution of particles is desired for achieving better wear behavior and mechanical properties. Homogeneous distribution of particles in a molten alloy is achieved due to the high shear rate caused by stirring the slurry and also stirring minimizes the particles settling [1, 2]. Fragmented dendrites are observed in the alloy matrix, although limited dendritic growth in the particle depleted region is also visible in the Fig.1 (b). Dendritic fragmentation can be attributed to the shearing of initial dendritic arms by the stirring action. During particle addition, there is some local solidification of the melt induced by the particles as there is a temperature difference between particle and the melt. It was also found that the perturbation in the

solute field due to the presence of particles can change the dendrite tip radius, and the dendrite tip temperature. These effects give rise to a dendrite– cell transition as the density of particles is increased. Also the length of the dendrite is reduced in the presence of the particles [1]. At higher magnification, optical micrograph shows that eutectic silicon exhibiting globular morphology and finely distributed as colonies around the reinforced particles as shown in Fig. 1(c). Particle clustering is observed in the micrograph Fig. 1(d) which is attributed to the particle pushing by solidification front. Fine particles are pushed or engulfed by the advancing Solid-Liquid interface during solidification [1].

The optical micrograph of SPS 2 reinforced with 15% coarse particles (106-125 μm) is shown in Fig.2. The Fig.2 (a) shows the homogeneous distribution of coarse particle in the alloy matrix. The mechanical stirring not only homogeneously distributes the particles but also delays the particle settling prior to solidification. Good bonding between particle and alloy matrix is exhibited in the Fig.2 (b). The smooth interface provides better mechanical and tribological properties as transfer of load is occurred though the interface. The long dendrite is observed in the Fig. 2(c), which is restricted by the particles. The second phase hard particle restrict the dendritic growth, the improvement in strength is caused by the refinement of the alloy dendritic array and is strongly linked to the more homogeneous distribution of second phases [2-6]. Fig 2(d) shows the distribution of silicon in the alloy matrix. The silicon possessing acicular morphology in the matrix but it colonizes in globular form in vicinity to the particle. Similar silicon morphology was reported in earlier work by kaur [7] and attributed this morphological transformation to the localized rapid cooling effect produced by zircon sand particle due large temperature difference in the melt around its vicinity

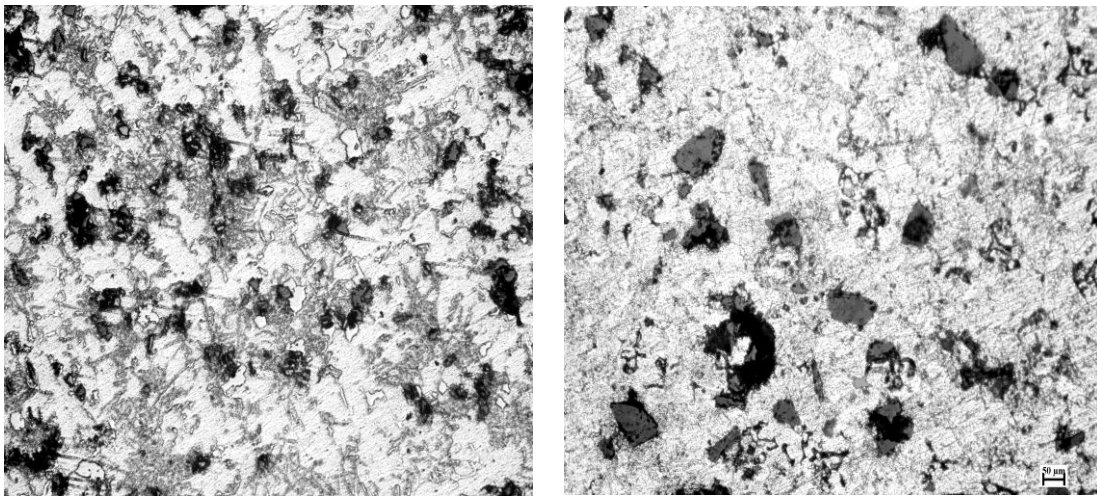
The optical micrograph of DPS 1 containing 12% coarse and 3% fine zircon sand particles is shown in Fig. 3. It depicts the homogeneous distribution of coarse and fine reinforced particles in the alloy matrix as shown in Fig.3 (a). The distribution of eutectic silicon becomes finer and some colonies of silicon are also visible in Fig. 3 (b&c). The optical observation clearly shows that, there is a better distribution of silicon in the matrix as compared to SPS 2 composite containing 15% coarse particles. Fig. 3(c-d) shows the uniform distribution of particle and silicon in the matrix.

Optical micrograph of DPS 2 composite containing 12% fine and 3% coarse zircon sand particles is shown in Fig.4. Homogeneous distribution of fine and coarse particles is depicted by the micrograph Fig.4 (a). Eutectic silicon acicular morphology is changed to globular and uniformly distributed throughout the matrix as shown in Fig. 4(b). The fine particles and silicon are arranged at grain boundaries and fragmented interdendritic region, some particles are engulfed within the primary grain. A network of silicon and fine particles are observed in the micrograph Fig. 4 (c-d). Minor amount of clustering is also there, as visible in the micrograph. Particle clustering can be explained by the fact that fine particles in composite are pushed to a greater extent by solidification front as compared to coarse particles. Most of the fine particles are placed at grain boundaries and very limited particles are engulfed within the grains. The particles are either pushed or engulfed by the solidification front [3]. Particle pushing and engulfing during solidification is also correlated with the mutual wetting behavior among the solid, liquid and particle phases. If the contact angle at a solid/liquid interface and a particle is less than 90° , the particle can be engulfed into the solid, and if the contact angle is greater than 90° , the particle would be pushed [4]. Coarse particles have greater tendency to settle as compared to fine particles, composite reinforced with coarse particle in majority are exhibiting clustering due to settling of particles and fine particles forms cluster by pushing action of solidification front [3, 4].



(a)

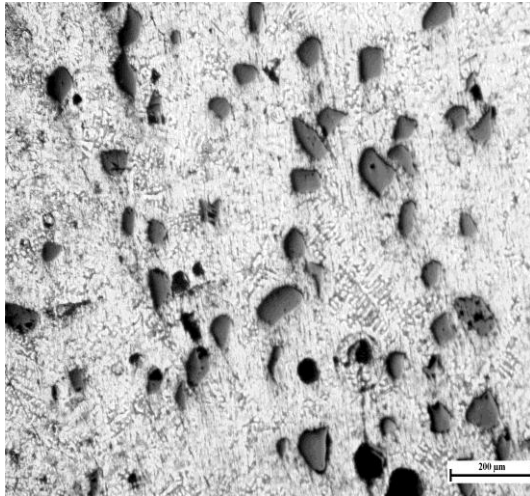
(b)



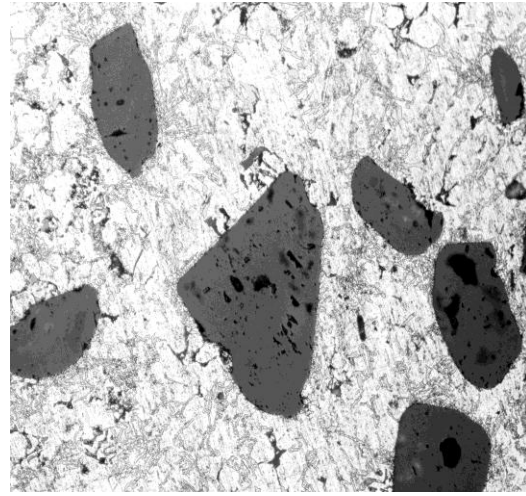
(c)

(d)

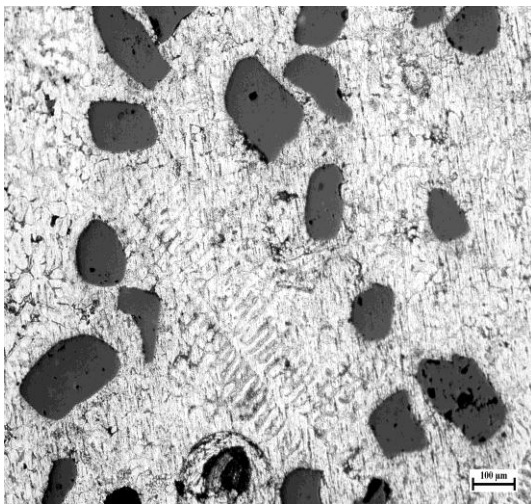
Fig.1. Optical micrograph of SPS 1 composites containing 15% fine particles (a) uniform particle distribution (b) micrograph showing dendritic growth in particle depleted region and many of dendrites are fragmented (c) eutectic silicon exhibiting globular morphology around particles (d) particle clustering is observed in the micrograph, primary silicon having less angular morphology and eutectic silicon colonizes around zircon sand particle.



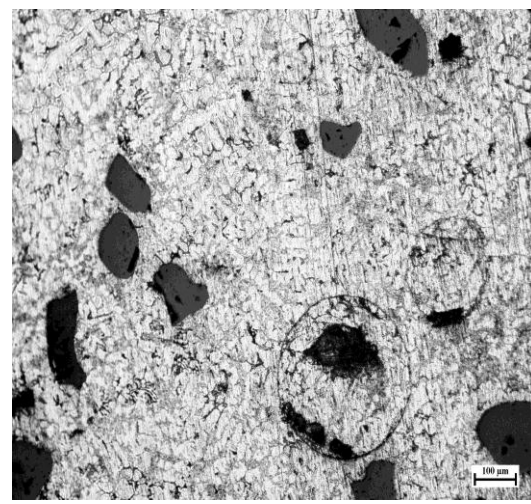
(a)



(b)



(c)



(d)

Fig.2. Optical micrograph of SPS 2 composites containing 15% coarse particles (a) uniformly arranged particles in the alloy matrix (b) consistent and better bonding between zircon sand particle and alloy matrix, eutectic silicon morphology changes from acicular to globular as it approaches to particle (c) long dendrite in particle depleted region and eutectic silicon nucleates between dendrite arm spacing (d) evenly distributed silicon in the matrix having acicular morphology and globular near the particles.

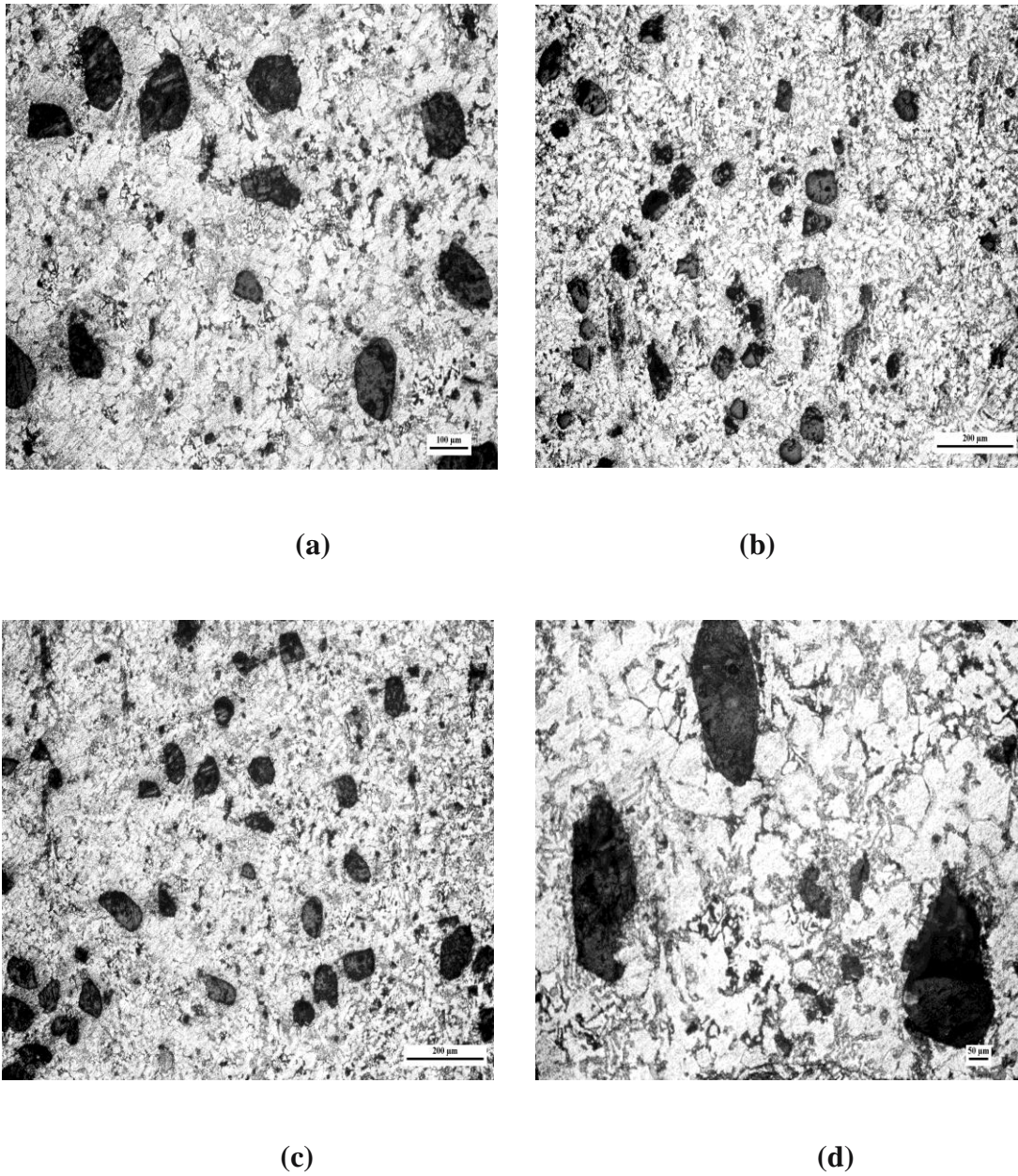
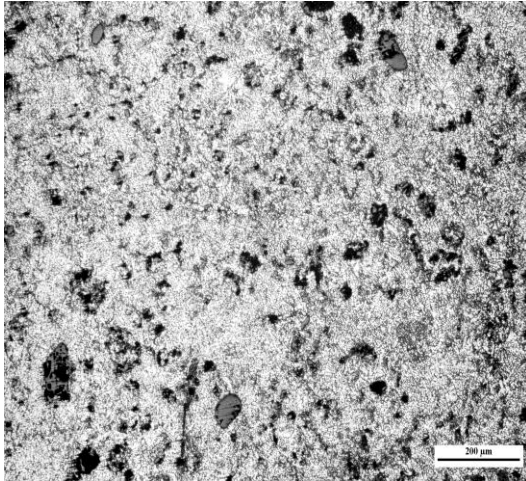
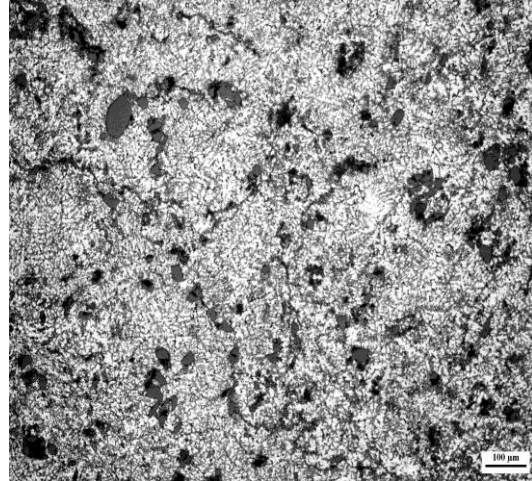


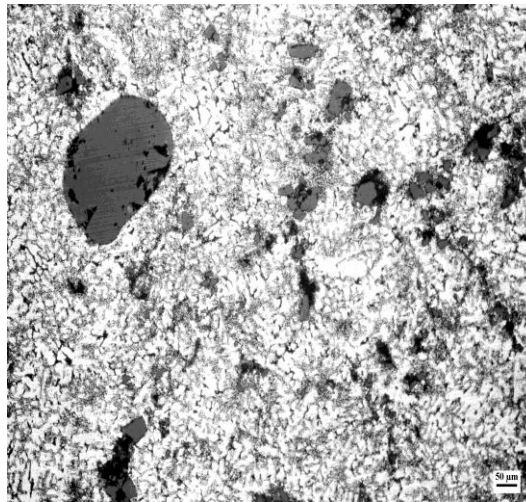
Fig.3. Optical micrograph of DPS 1 composites containing 12% coarse and 3% fine particles (a) coarse and fine particles are uniformly arranged in the alloy matrix (b) eutectic silicon morphology changes from acicular to globular in vicinity to particle (c) silicon is of globular morphology and distributed dense near the particle (d) good bonding between zircon sand particle and alloy matrix



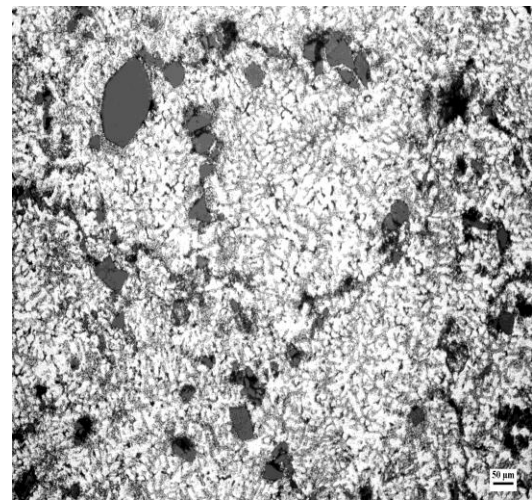
(a)



(b)

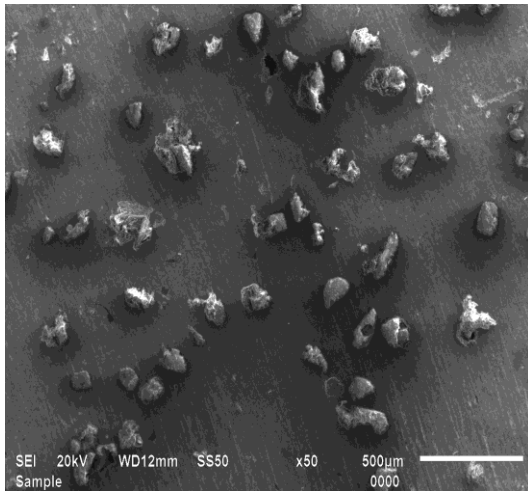


(c)

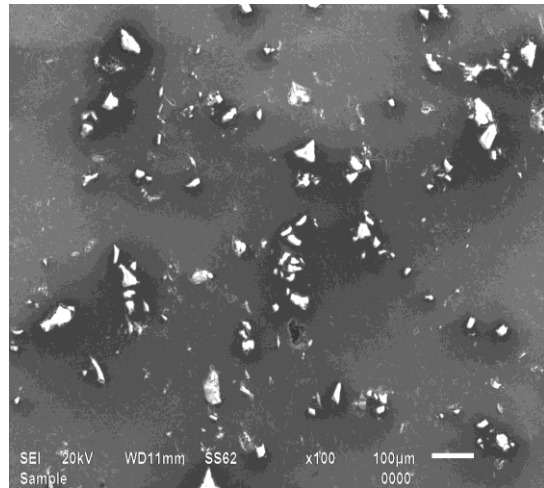


(d)

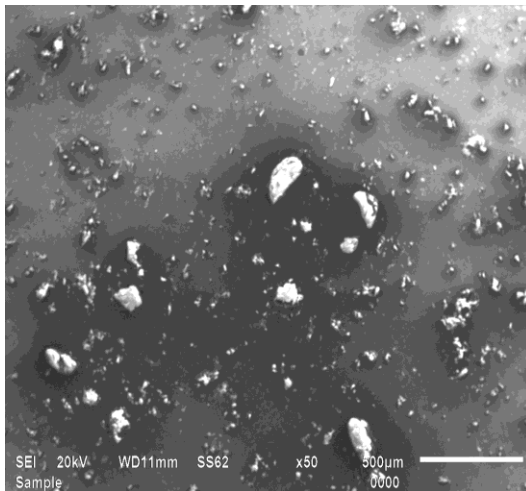
Fig.4. Optical micrograph of DPS 2 composites containing 12% fine and 3% coarse particles (a) homogeneous distribution of coarse and fine particles in the alloy matrix (b) silicon traps in interdendritic region (c) good bonding between zircon sand particle and alloy matrix (d) fine particles showing clustering.



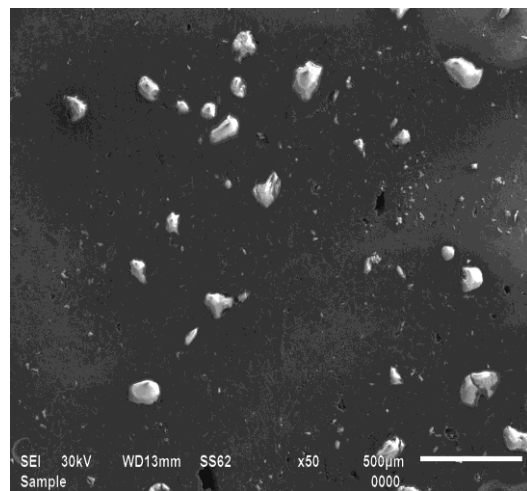
(a)



(b)



(c)



(d)

Fig.5. SEM micrograph of composites showing the homogeneous distribution of coarse and fine particles. (a) SPS 1 (b) SPS 2 (c) DPS 1 (d) DPS 2.

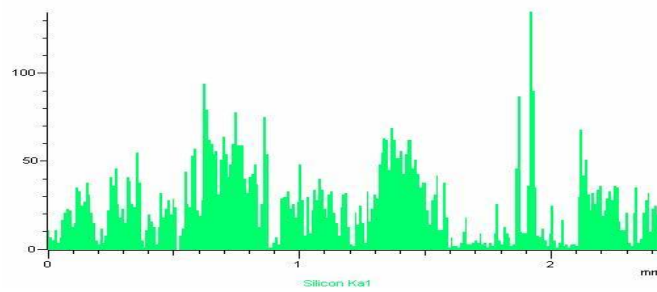
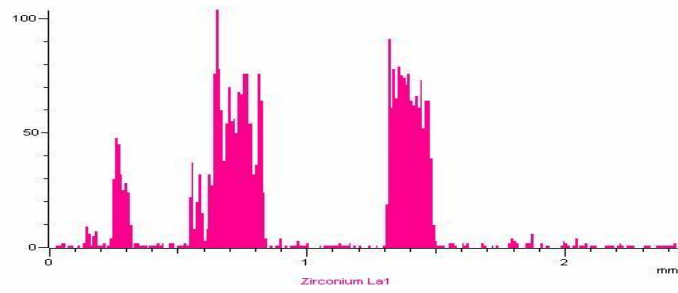
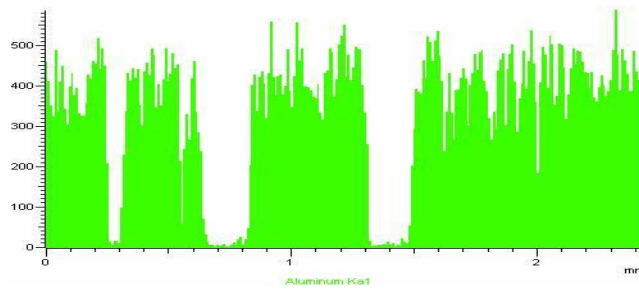
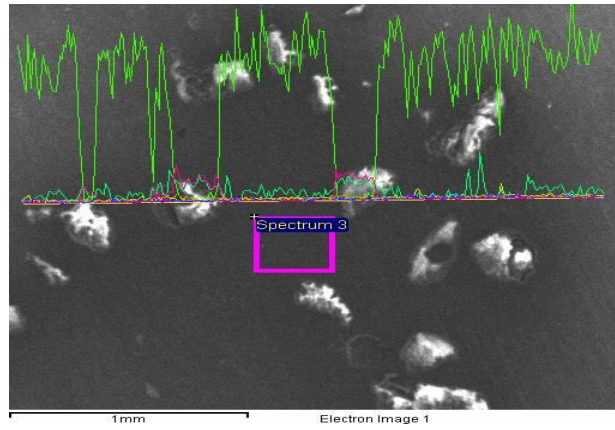


Fig 6. Line profile of composite

4.2 Line Profile Analysis:

Line profile analysis of the composite clearly shows the presence of silicon in vicinity to the zircon sand particle. Silicon is uniformly distributed throughout the matrix but its concentration is higher near to zircon sand particle as shown in Fig.6.

4.2.1 EDS Analysis:

The EDS analysis of zircon sand particle of reinforced composite is given in Fig. 7 shows the presence of silicon on zircon sand. It confirms that zircon sand particle provides a nucleating site for silicon.

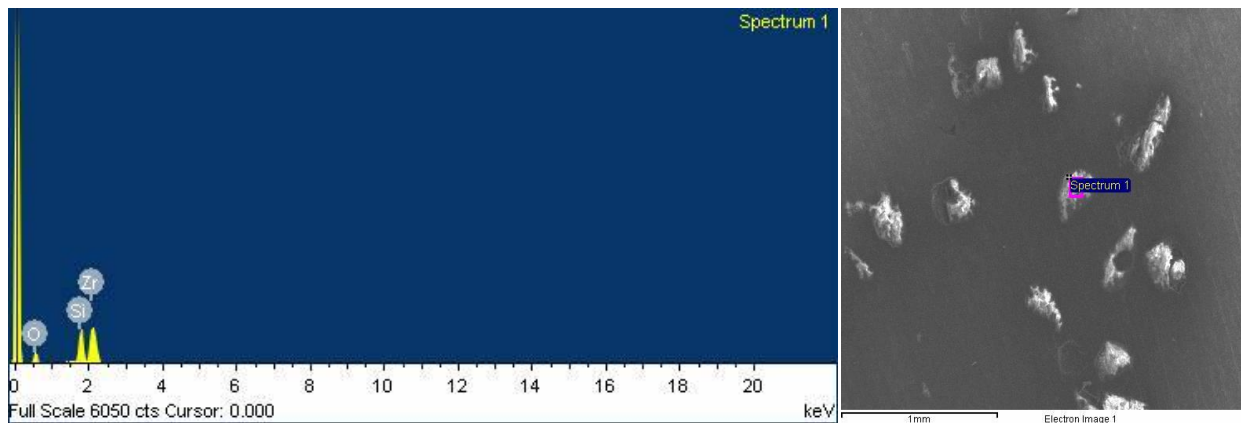


Fig.7. EDS analysis of embedded Zircon sand particle in alloy matrix

4.3 Hardness

The microhardness measurement at different phases of composites has been carried out to know the effect of reinforced particulates on the alloy matrix. Which is given in table V. Microhardness measurement have been carried out on the embedded zircon sand particles

Table IV-Variation of hardness at different phases

Composite	Microhardness (Hv)		
	At Particle	At Interface	At Matrix
SPS 1	709	123	88.6
SPS 2	736	103	82.1
DPS 1	716	102	79
DPS 2	719	116	81

as well as in the vicinity of particles and matrix. Zircon sand particles show high hardness which decreases as we move away from particle. The high hardness at particle/matrix interface indicates good bonding microhardness in comparison to coarse particle size zircon sand reinforced composite at interface and matrix. Between particle and alloy matrix fine particle size zircon sand reinforced composite shows better microhardness in comparison to coarse particle size zircon sand reinforced composite at interface and matrix.

4.4 Wear characteristics

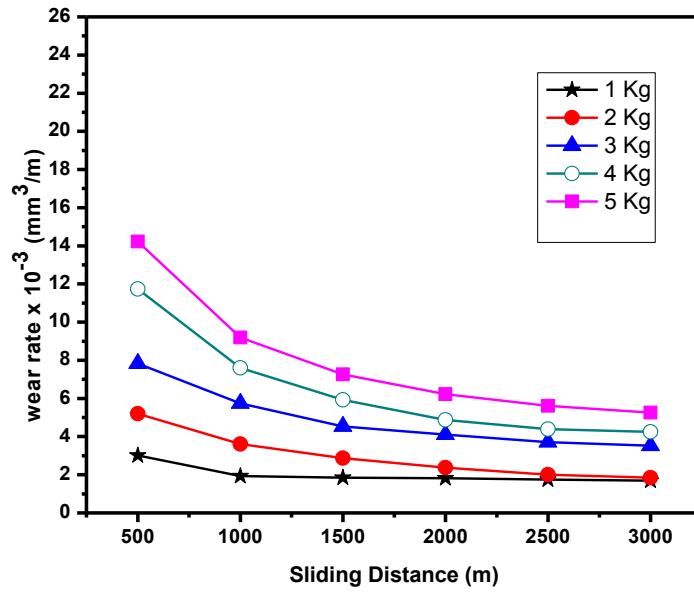
4.4.1 Effect of sliding distance on wear rate

The wear rate behaviors against sliding distance of the composite has been investigated at five different loads at room temperature which is shown in Fig.8. It can be found clearly from the graph that the wear rate of the composites increases with the increase in applied load. The curve reveals two different type of wear behavior under an applied load. The steep in the initial stage give rise to greater wear corresponding to the run in wear. However, steady state wear is obtained in the later stage. Moreover, with increase in load the run-in and steady state wear rate are also found to increase. These results are analogous to results reported earlier under similar sliding conditions by Kaur et al. [7] for spray formed zircon sand reinforced composite and Chaudhury et al. [10] for stir cast Al-2Mg-11 TiO₂composites.

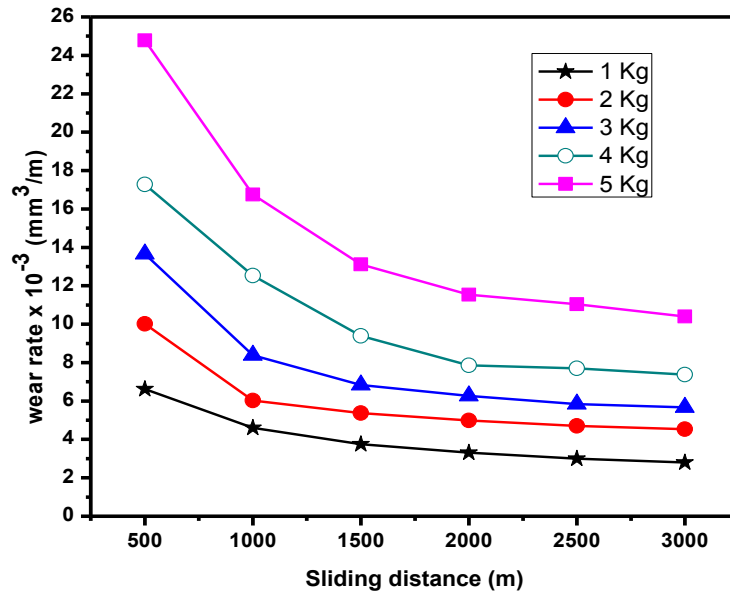
The wear behavior of SPS 1 presented in Fig. 8 (a) shows that steady state wear is approachable after 1000 m sliding distance. While in SPS 2 as shown in Fig. 8 (b) steady state wear is delayed and occurs after sliding distance of 1500 m at low loads, on high loads the steady state wear is approachable at 2000 m sliding distance. Run-in wear of SPS 2 is higher as compared to SPS 1 composite as shown in Fig. 8 (a-b). This indicates that fine particle reinforced composite exhibits better wear resistance as compared to coarse particle reinforced composites. These results are in good agreement with the earlier reported results [8, 9].

To study the effect of inverse particle size addition i.e. fine particle addition in coarse particle reinforced composite and vice-versa, the wear rate comparison of SPS 2 and DPS 1 as shown in Fig. 8 (b-c) clearly shows that addition of 3% fine particles to coarse particle exhibits better wear properties as compared to only coarse particle reinforced composite. There is decrease in wear rate at all loads, not only wear rate but run-in wear also reduces to greater extent and steady state wear approaches at earlier sliding distance. On the other hand, comparing the coarse particle addition to fine particle with fine particle reinforced composite i.e. SPS 1 and DPS 2 gives different results as shown in Fig. 8 (a, d), the graphical

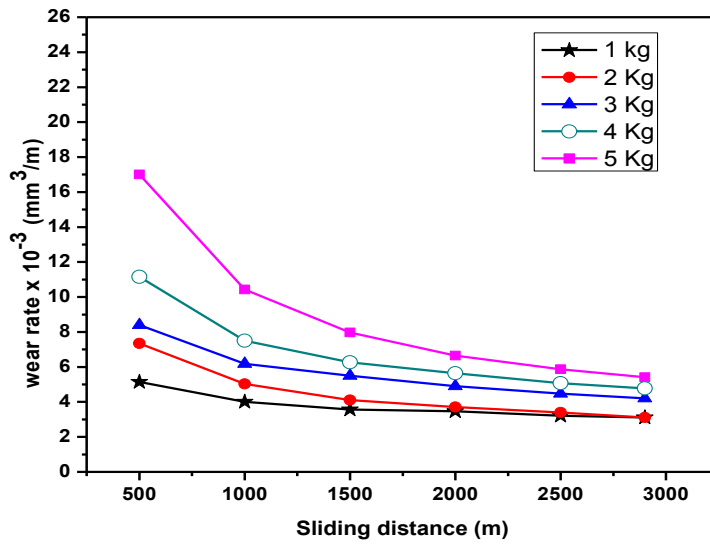
presentation reveals that coarse particle addition marginally increases the wear rate as compared to single size fine particles reinforced composite, but run-in wear is slightly lesser. It can be concluded after graphical study that fine particle addition in coarse particle reinforced enhances the wear properties, while coarse particle addition to fine particle reinforced composite not work well to enhance the wear properties. As reported earlier, the coarser particles help to carry a greater portion of the applied load, thereby reducing the load on the finer particles as well as on the base metal. In addition, the coarser particles in the DPS composites could help to shield the finer particles from the gouging action of the abrasive thus, helping the smaller particles to continue performing their wear resisting function longer than in SPS composites. This can be attributed to the fact that, less quantity of coarser particles are unable to shield the fine particles and also chipping off coarser particle during adhesive wear pulls out the finer particles along with them at higher load. It is confirmed by the result as mentioned earlier, in which 12% coarse zircon sand particles and 3% fine zircon sand particles gives better wear resistance.



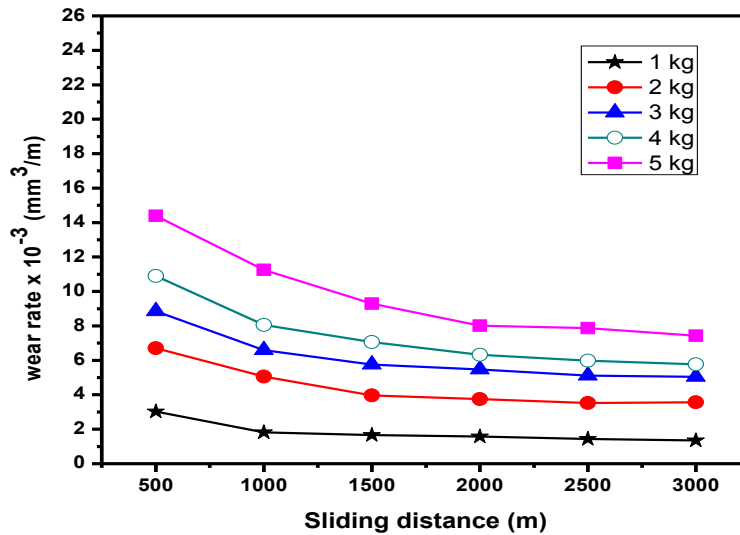
(a)



(b)



(c)



(d)

Fig.8. Wear rate of composites against sliding distance at different loads (a) wear rate of SPS 1 LM13/ 15% Zircon sand fine particles [20-32 μm] (b) wear rate of SPS 2 LM13/ 15% Zircon sand fine particles [106- 125 μm] (c) Wear rate of DPS 1 LM13/ 15 % zircon sand[12%C +3%F] (d) Wear rate of DPS 2 LM13/ 15 % zircon sand [12%F +3%C].

4.4.2 Effect of load on wear rate

The bar graph of wear rate comparison of composites with different load is presented in Fig 9. In Fig. 9 (a), the graphical representation clearly shows the wear rate of coarse particle reinforced composite i.e. is SPS 1 is higher as compared to fine particles reinforced composite i.e. is SPS 2 on all investigated loads. Further on low and high loads the wear rate of SPS 1 nearly double as compared to SPS 2, wear rate difference is less between the composites at load range of 3-4 kg. This representation concludes that fine particle reinforced composite exhibits better wear resistance in comparison to coarse particles. Similar results are reported earlier by various researchers [8, 9].

The Fig. 9(b) shows that, the wear rate of DPS 2 is higher than SPS 1 composite at all investigated loads. Graphical study clearly depicts that, the coarse particle addition in fine particle reinforced composites is not effective in enhancing the wear resistance of the composite. It is not the case in the composite with fine particle addition to the coarse particle reinforced composite as presented in the Fig. 9 (c). SPS 2 containing 15% coarse particle shows higher wear rate in comparison to DPS 1 reinforced with 12% coarse and 3% fine zircon sand particles. The fine particle addition enhances the wear resistance of the coarse particle composite at all investigated loads. It is concluded from the Fig9. (b-c) that fine particle addition in coarse particle reinforced enhances the wear resistance of the composite but coarse particle addition to fine particle reinforced composite increases the wear rate.

The graphical comparison of composites SPS 1, SPS 2, DPS 1 and DPS 2 depicts that, the composite reinforced with 15% coarse particle i.e. SPS 2 exhibits higher wear rate at all investigated loads. At higher load the difference between wear rates of SPS 2 as compared to other composites is greater, which is lesser at low load.

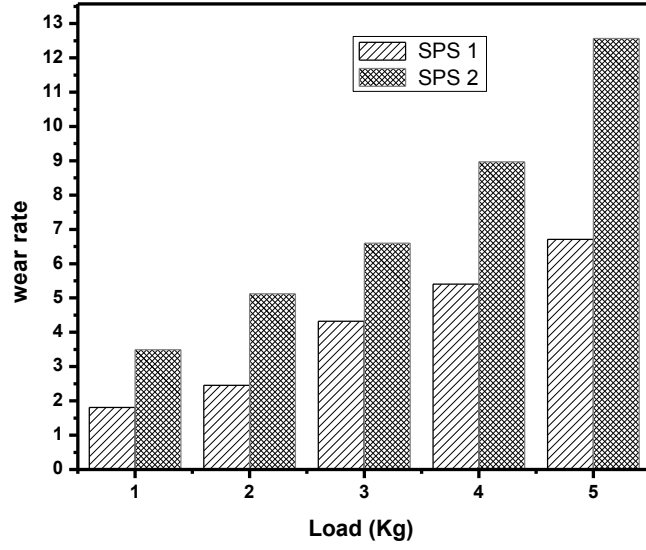
The graphical presentation of wear rate of the composites on different loads is shown in Fig.10. The Fig. 10 shows the wear rate of SPS 1, SPS 2, DPS 1 and DPS 2 on different loads i.e. 1-5 Kg. The wear follows a linear relationship with respect to increasing load which

portrays Archard's law of adhesive wear for metals. It clearly shows that, SPS 1 exhibiting better wear resistance as compared to all composites under investigation.

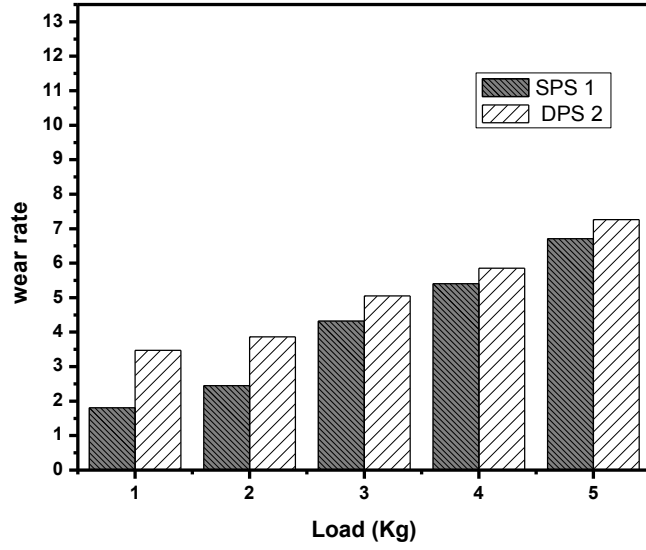
The wear rate results of SPS 1 shows a change in slope of wear curve from 2 kg to 3 kg load. This change in slope corresponds to the change in wear behavior from mild to severe behavior. On the other hand the transition from mild to severe behavior in SPS 2 occurs from 3 kg to 4 kg load. The severe wear manifested itself by massive surface damage and large scale matrix material transfer to the counterface accompanied by the generation of coarse debris particles, typically in the shape of plates with a shiny metallic appearance. Similar results are reported earlier by Kaur et al. [7] for spray formed zircon sand reinforced LM 13 composite i.e. same alloy and size of reinforcement as used in this study.

To compare the effect of dual size particle on wear rate against load, the graph shows that DPS 1 exhibits better wear resistance by only addition of 3% fine particles as compared to SPS 2 composite, which contain only coarse particle of single size. The fine particles works effectively to resist wear and there shielding is done by the coarse particles [6]. Comparing the SPS 1 and DPS 2 depicts that, the coarse particle addition to fine particles adversely affect the wear properties as shown in Fig. 10.

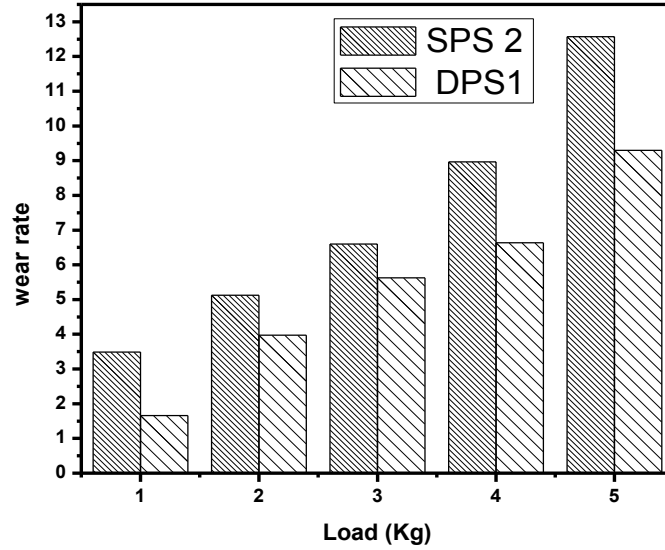
The wear mechanism can be further explained well by analyzing the microstructural features of the worn surface of pin and the wear debris.



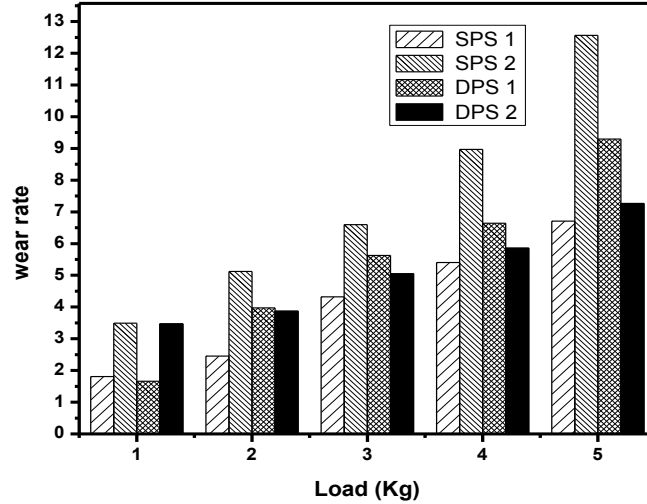
(a)



(b)



(c)



(d)

Fig.9. Bar graphical presentation of Wear rate at different loads (a) wear rate comparison of SPS 1 and SPS 2 (b) wear rate comparison of SPS 1 and DPS 2 (c) wear rate comparison of SPS 2 and DPS 1 (d) wear rate comparison of SPS 1, SPS 2, DPS 1 and DPS 2.

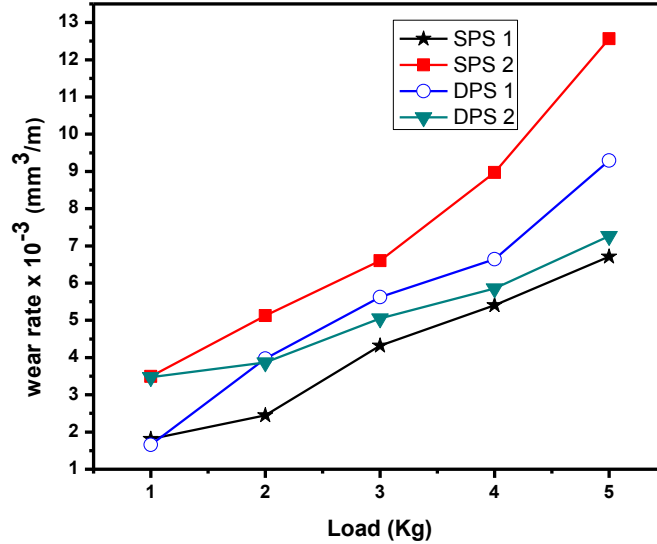


Fig.10. Wear rate of composites at different loads

4.4.3 Morphological analysis of worn surface and debris

The morphologies of worn out surface of pins and debris offer clues to the wear mechanisms involved in sliding the sample against load. The Scanning electron microscope (SEM) micrographs of the single and dual size zircon sand reinforced composites tested at loads of 1-5 kg at a speed of 1.61 m/s are presented in Fig. 11, which show the wear track morphology of the specimens tested.

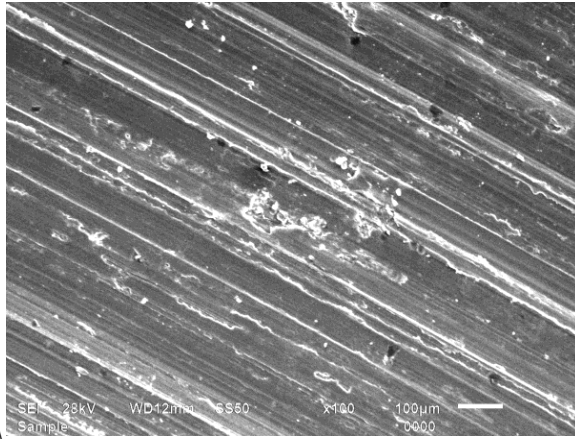
One of the common feature observed in both lower and higher load, is the formation of grooves and ridges running parallel to the sliding direction in composites. On further analyzing it has been found that wear grooves are fine in worn pin surface of composite subjected to low load as compared to high load. The depth of microploughing is increased on increasing load to 5 kg where contact asperities change the shape. Consequently the size and depth of the grooves become greater at this stage. However, at high loads the worn surfaces in some places reveal patches from where the material was removed from the

surface of the material during the course of wear. Similar morphology of wear track at worn out surface of pin are observed earlier in previous work reported by Sharma et al. [12] and kaur et al. [7].

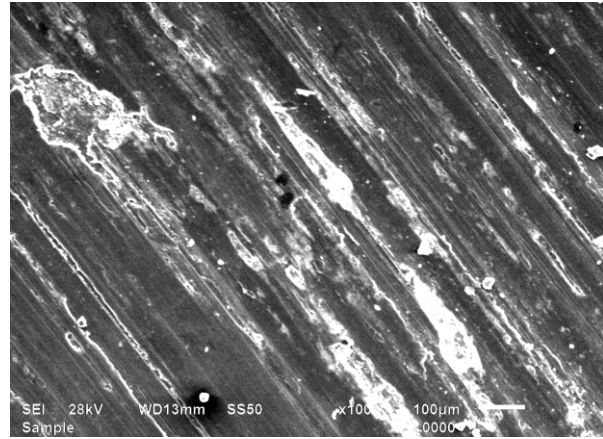
The Fig. 11 (a) shows the SEM micrograph of worn pin SPS 1 composite reinforced with fine size zircon sand particles at load of 1kg. At low load as shown in micrograph, the worn surfaces are smooth and ploughing strips are very shallow on the surface. At 2 kg load, the ploughing marks got deeper as shown in Fig. 11 (b) and damaged spots in the form of craters can be seen, which will grow further in size on increasing load. Particle cracking and microcrack are observed at higher magnification shown in Fig. 11 (c), these factor increases the wear rate significantly. This behavior is characterized as severe wear behavior, in which material removal is accelerated.

The material of the pin adheres along the flat running surfaces causing adhesive sliding wear as shown in Fig. 11 (d) at 3 kg load. This wear behavior causes the damage to parent material and wear rate increases significantly. The crack running from the removed material is also visible in the matrix and loosely held debris flakes, which may detach further on higher load.

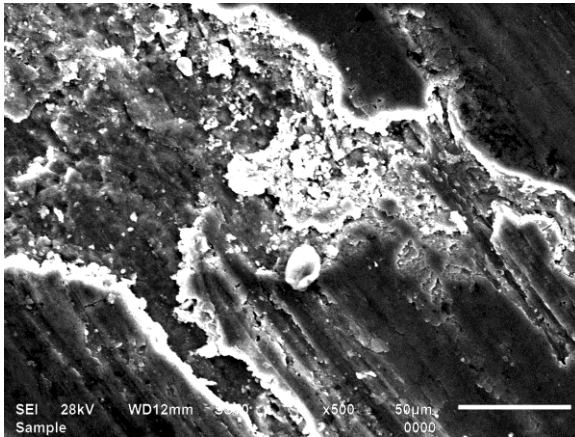
At 4 kg the material removal increases significantly and the cross section of the craters increases as shown in Fig. 11 (e). At 5 kg load material removal rate is significantly higher, adhesive wear is dominating at this stage. Microcracks results in delamination, which in turn damage the parent material by excessive material loss. The loose wear debris and crushed zircon sand particles are seen on the wear track as shown in Fig. 11 (f)



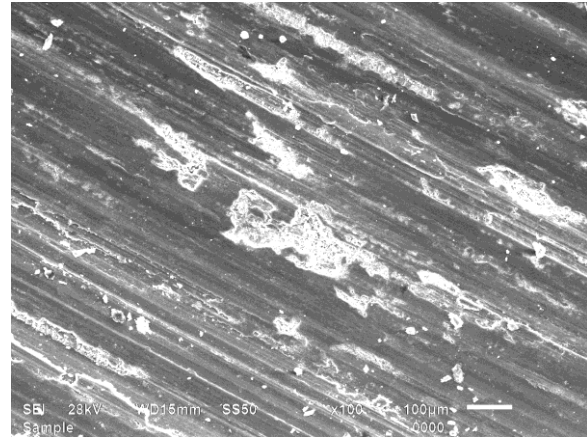
(a)



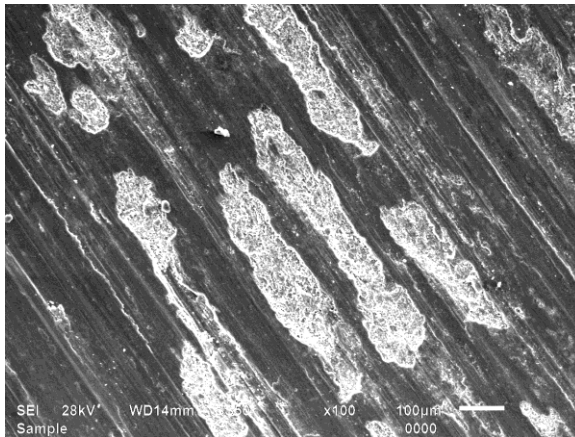
(b)



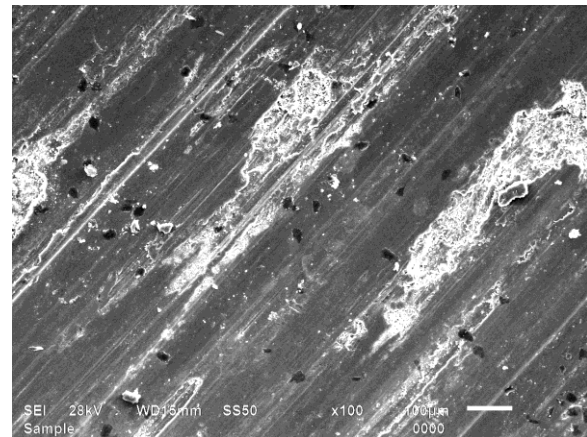
(c)



(d)



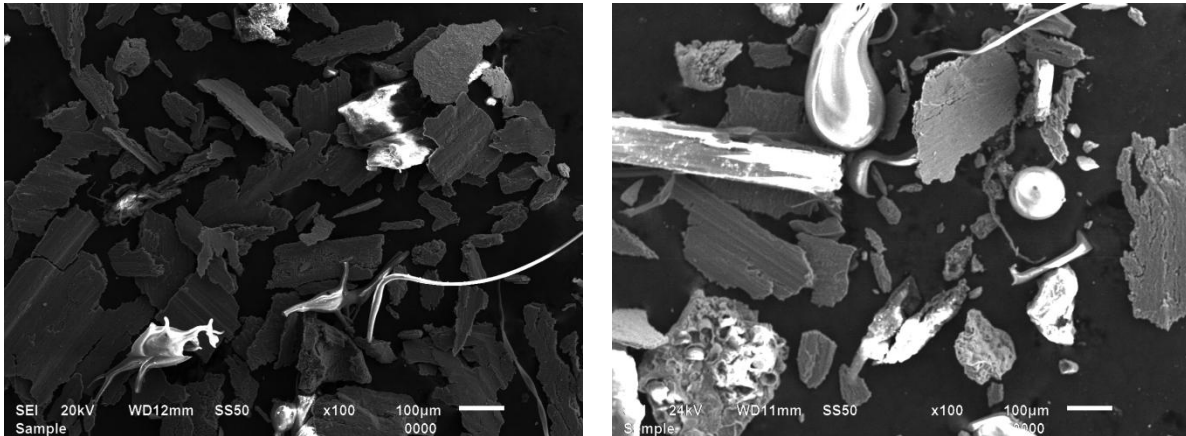
(e)



(f)

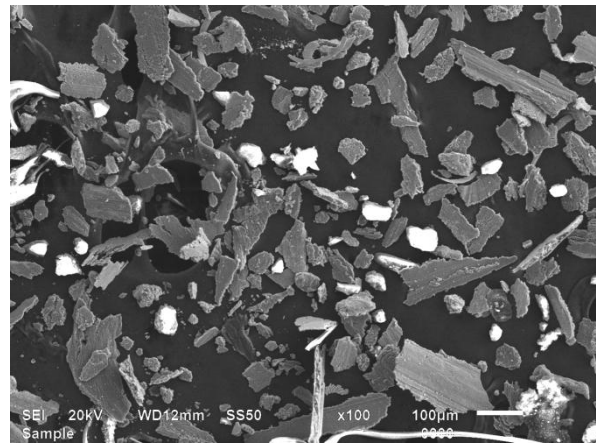
Fig.11. SEM micrograph of worn out surface of SPS 1 composite at different loads (a) 1kg (b) 2kg (c) higher magnification at 2kg (d) 3kg (e) 4kg (f) 5kg

Wear debris generated at higher load of SPS 1 are presented here in Fig. 12. Fig. 12(a) shows wear debris obtained at 3 kg load in which plate like debris of matrix alloy and debonded zircon sand particles are observed. Wear is governed by delamination, which gives plates like morphology of debris with microcracks.



(a)

(b)



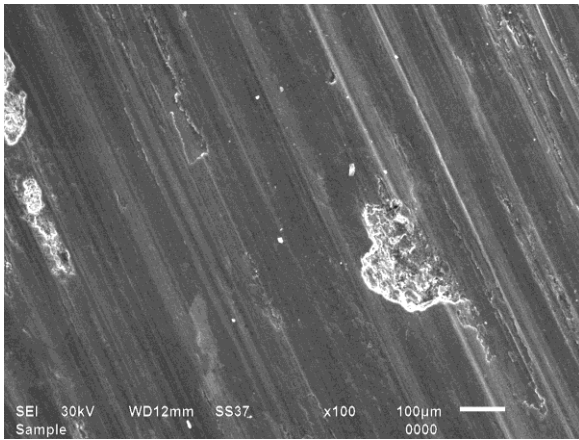
(c)

Fig.12. SEM micrograph of Wear debris generated of SPS 1 at (a) 3kg (b) 4kg (c) 5kg

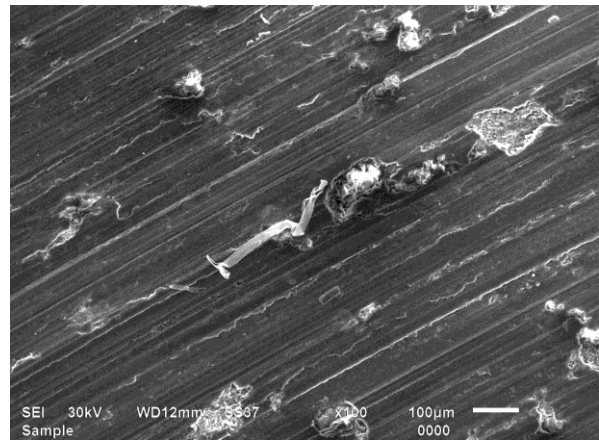
Wear debris at 4 kg load as shown in Fig. 12 (b) shows the plate or flakes of alloy matrix and debonded zircon sand particle spheroidizes as they are trapped in sliding action. The debris particles are likely to act as the third-body abrasive particles and could be responsible for the higher wear rate. Loose debris particles trapped between the specimen and the counterface causes a microploughing on the contact surface of the composite.

Debris flakes having cracks and majority of flakes having number of cracks due to repetitive stress occurred in sliding under high load. When the load is increased, the dominant wear mechanism becomes to delamination and severe plastic deformation. Wear debris generated at 5kg load as shown in Fig 12 (c) having long flakes by delamination and small flakes, small flakes are generated by the crushing of the flakes at high load. Debris having long flakes as compared to debris generated at low load, which depicts the severe wear behavior.

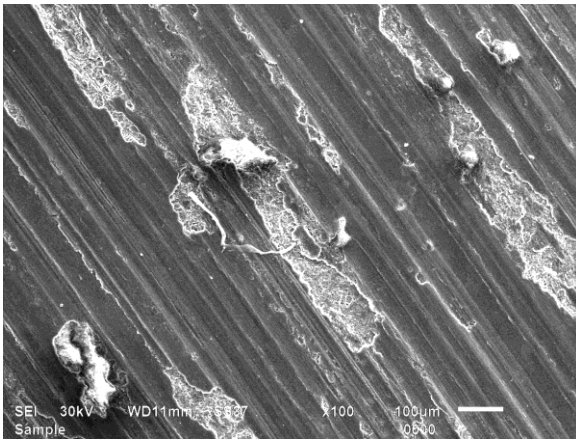
Worn out pin surface SEM micrograph of SPS 2 are presented in Fig 13. Fig. 13(a) shows worn surface at 1 kg load in which grooves and ridges running parallel to the sliding direction. Microploughing is dominating wear mechanism although local damaged spots are also observed on the surface. At 2 kg load the grooves are distinct and deeper, crater grow in size which exposes the reinforced particles as shown in Fig. 13 (b). As load increases the adhesive wear mechanism operates and removes the ductile matrix material. The particle are protruding in the matrix depicting good bonding between particle and alloy matrix as observed in Fig. 13 (c). At high load the material removal is governed by adhesive wear and crack propagation resulting in delamination of matrix material. The protective layer of the reinforcing particles can no longer remain stable under the ploughing action at high load. The material removal is enhanced by adhesive wear mechanism and numbers of craters are increased between deep ploughing marks as shown in Fig. 13(d-e). Material removal during the process is in the form of small pieces resulting in the formation of flake-type debris. As shown in Fig. 13 (f), the craters are so large and distinct that the surface underneath is visible. The higher magnification SEM examination at 5 kg load of the subsurface clearly reveals cracks indicating delamination wear.



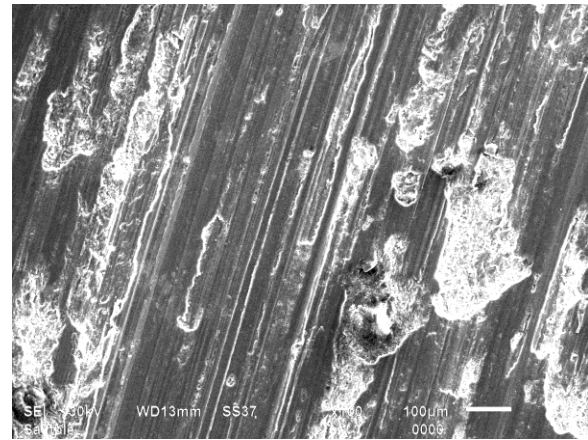
(a)



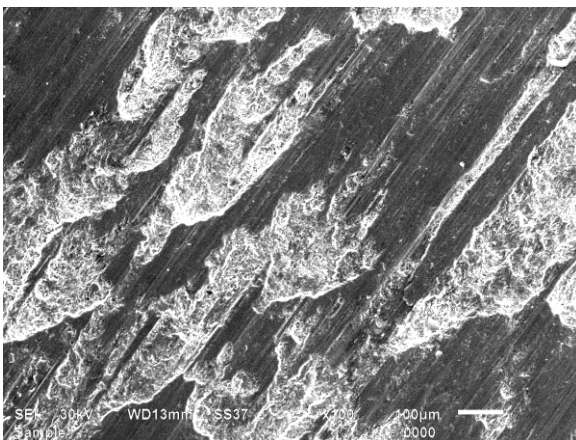
(b)



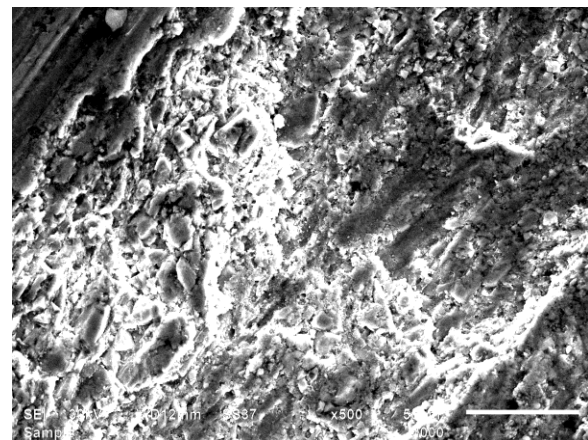
(c)



(d)



(e)



(f)

Fig.13. SEM micrograph of worn out pin surface of SPS 2 composite at different loads (a) 1kg (b) 2kg (c) 3kg (d) 4kg (e) 5kg (f) higher magnification at 5 kg

Wear debris of SPS 2 composite is shown in Fig. 14. The debris obtained at 1 kg load is of plate like morphology and zircon sand particle is not observed, which indicates that, the reinforced particles bearing the load while ductile matrix alloy generated plate like debris as shown in Fig. 14 (a). As load increases the debonding of zircon sand particles occurs and long flakes of debris having different morphological appearance as observed in Fig. 14 (b).

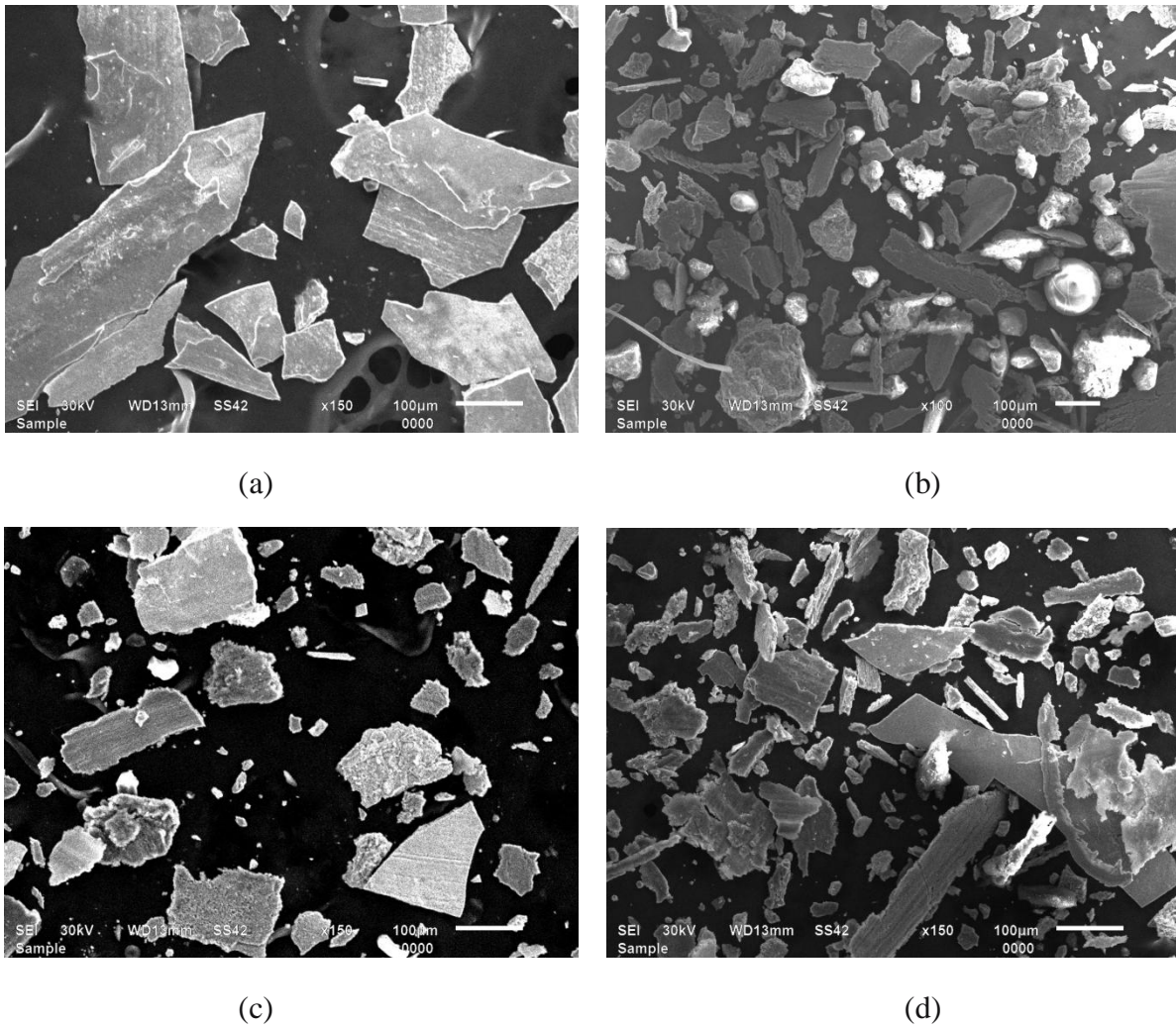
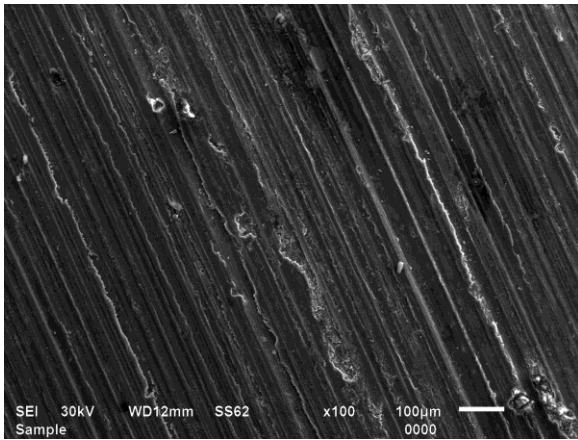


Fig.14. SEM micrograph of Wear debris generated of SPS 2 at (a) 1 kg (b) 3kg (c) 4kg (d) 5kg

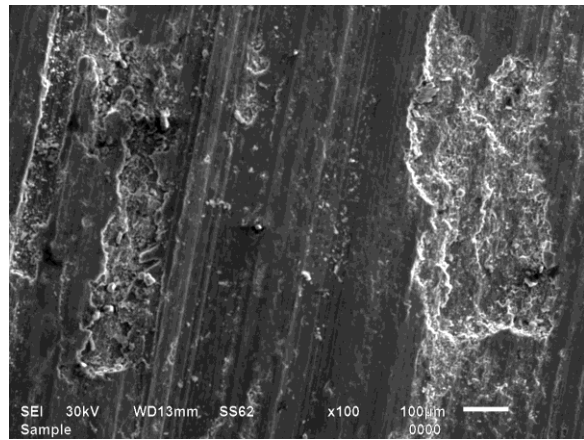
In the collected wear debris zircon is present in mechanically mixed layer form. The particle itself has cracked into further smaller fragments and after long run it is making an oxide rich layer on the worn surface by picking iron oxide from the counterface.

This is confirmed by EDS analysis which shows iron content even more than alloy matrix as shown in Fig. Several microcracks are there in debris indicating delamination while zircon sand particle takes spherical shape by trapping in due course of sliding. Twisted and layered debris revealing the repetitive nature of stress occurred at high load sliding condition. At 4kg load as shown in Fig. 14(c) the debris having long flakes apart from this small metallic debris are also observed, which may be fragmented during sliding action. Debris at 5kg load shows mixed morphology with long flakes, small fragmented flakes and layered flakes. Crack propagation leads to delamination although some flakes also depicting microcutting behavior as shown in Fig. 14 (d).

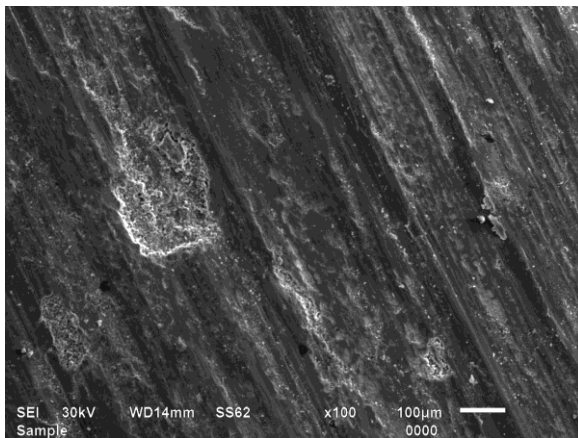
Fig. 15 shows the pin surface morphology of DPS 1 composite. At 1 kg load, the grooves running all over the pin surface along sliding direction as shown in Fig. 15(a). Load increment initiates the crater and crack formation, as shown in Fig. 15(b) at 2kg the crater formation starts by the loss of parent material . The rupture of mechanically mixed layer initiates the adhesive wear mechanism and crater grows in size at 3 kg (Fig. 15(c)). At 4kg load the material removal shows the dimple like morphology, as void nucleates around the particle in the ductile matrix as observed in Fig. 15(d). At higher load i.e. at 5kg the cracks propagates and removal of material occurs by delamination as shown in Fig. 15 (e). A lower magnification micrograph shows the dimple morphology around the particle (Fig. 15 (f)).



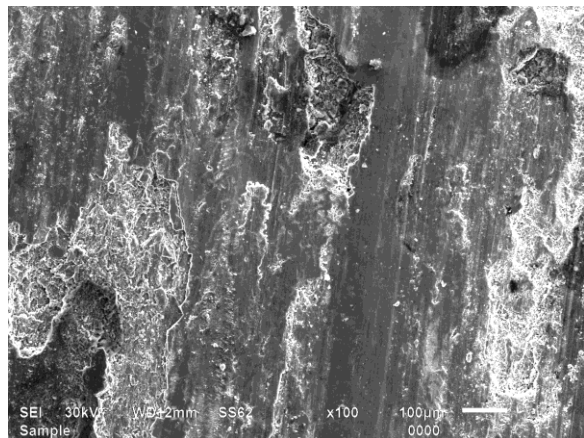
(a)



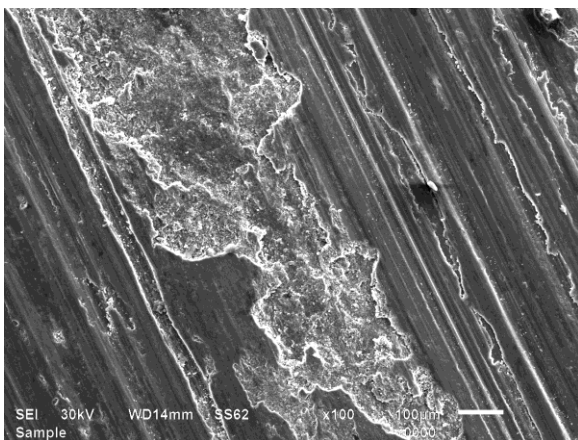
(b)



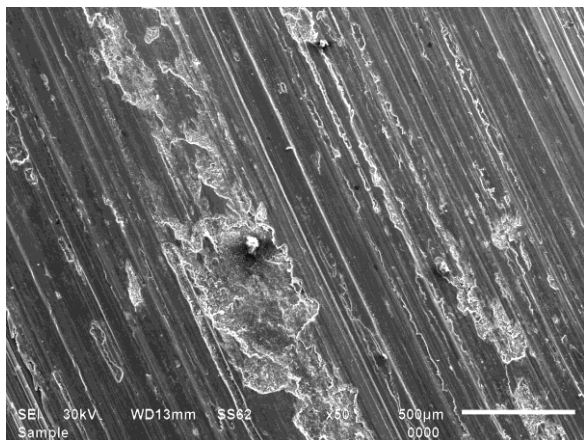
(c)



(d)



(e)



(f)

Fig.15. SEM micrograph of worn out pin surface of DPS 1 composite at different loads (a) 1kg (b) 2kg (c) 3kg (d) 4kg (e) 5kg (f) lower magnification at 5 kg

Wear debris of DPS 1 composite are presented in Fig. 16. The long flakes with microcracks along with debonded zircon sand particle are observed in debris collected at 3 kg load as shown in Fig. 16(a). At higher load i.e. 5kg load, the flakes having number of microcracks and flakes edge reveals that cracks are responsible for their delamination from the parent material. Some flakes having embedded particles, which are pull out with the parent material due to excessive plastic deformation as shown in Fig. 16 (b).

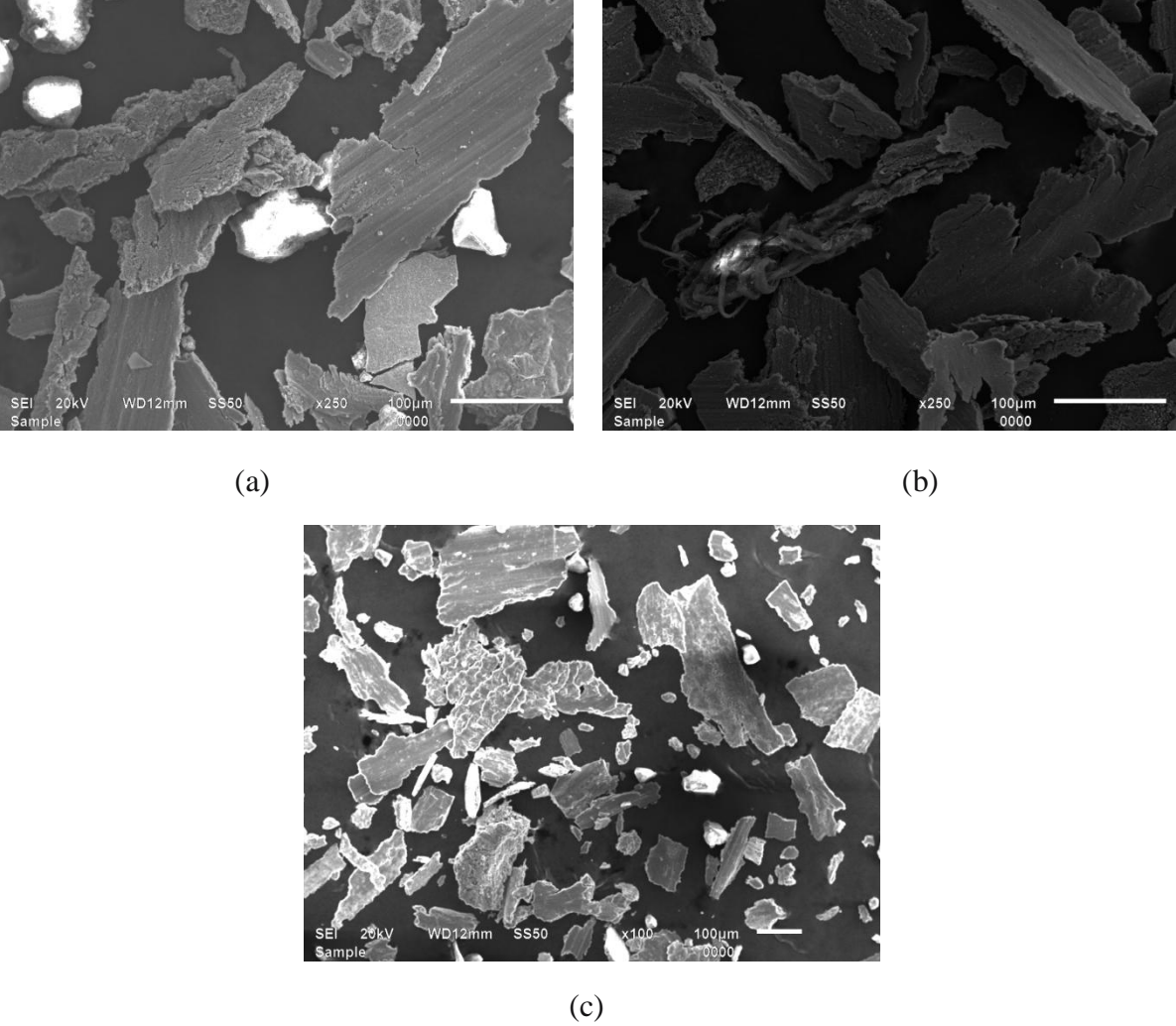
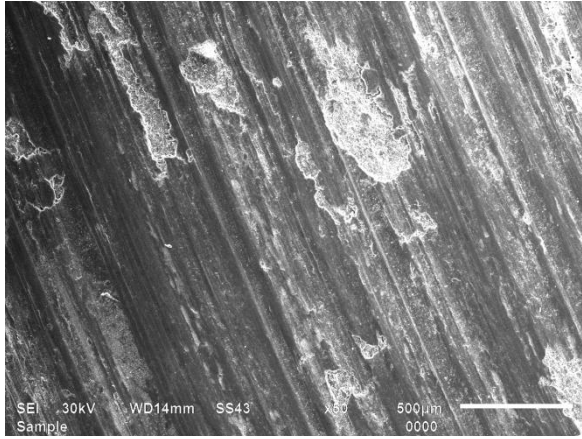


Fig.16. SEM micrograph of Wear debris generated of DPS 1 at (a) 4kg (b) 5kg (c) 3kg

Wear debris generated at 3 kg load at higher magnification show corrugated and layered structure as shown in Fig. 16 (c). The steps or layered structure observed could be due to rubbing caused by constant sliding between the pin material and counterface. Each of the steps could then be caused by the deforming force subjected in one rotation. Similar wear debris morphology is earlier reported by Bakshi et al. [13] for aluminum-silicon composite coatings prepared by cold spraying.

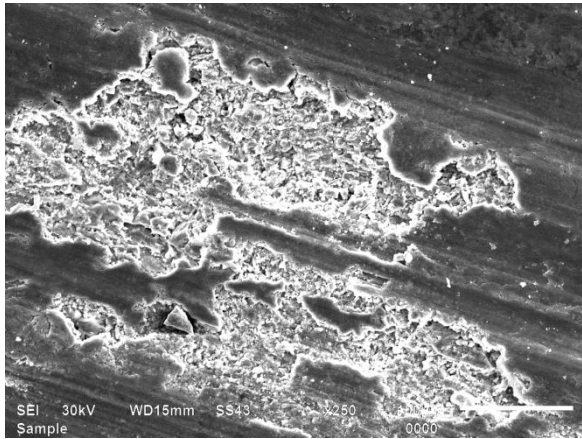
Worn surface of DPS 2 is examined by SEM is presented in Fig.17. Fig 17 (a) shows the worn surface at 1 kg load, the excessive ploughing action is observed as the grooves are deeper at low load as compared to other composite in this study. Crater's also originated on the surface having several microcracks at the edge perpendicular to the sliding direction. At 2 kg load, the particles are exposed as parent material is removed by adhesive wear mechanism as shown in Fig. 17 (b). The excessive deformation causes the crater to grow in size and the edge having cracks, which causes delamination. Some loosely held debris originated by the cracks can be clearly seen in the micrograph Fig. 17 (c). At 4 kg load, the material removal is excessive as Fig. 17(d) shows that materials along with particles are removed by delamination. The grooves are again formed on the worn surface as seen in the micrograph. At 5kg load the crack propagation lead to excessive removal of parent material although some island type parent material remains there, as they bypass the crack growth as shown in Fig. 17(e).



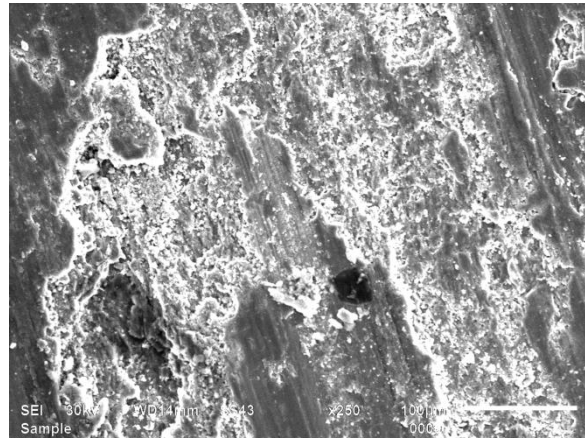
(a)



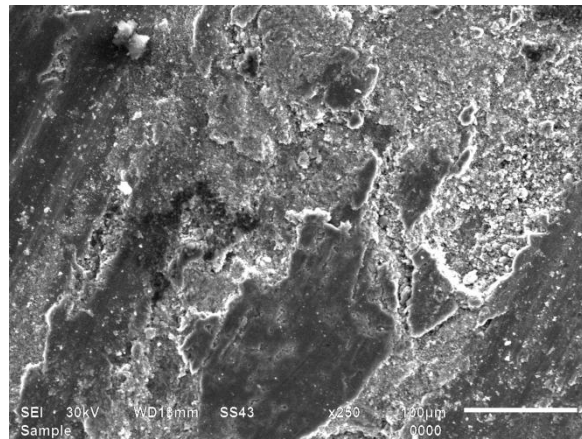
(b)



(c)



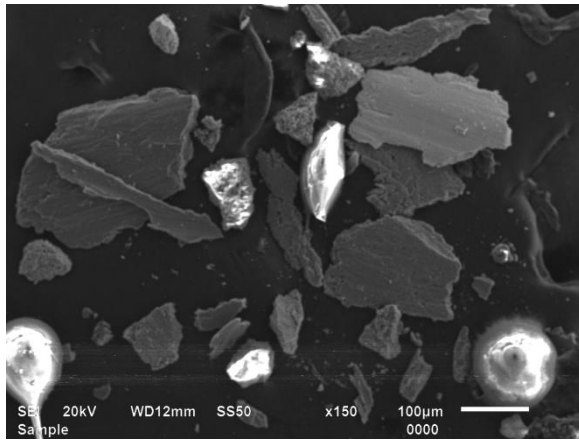
(d)



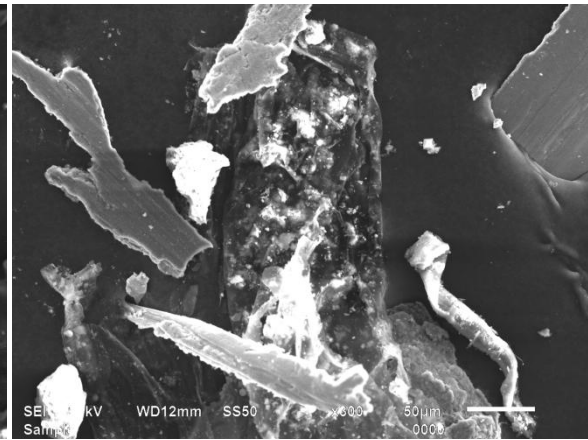
(e)

Fig.17. SEM micrograph of worn out pin surface of DPS 2 composite at different loads (a) 1kg (b) 2kg (c) 3kg (d) 4kg (e) 5kg

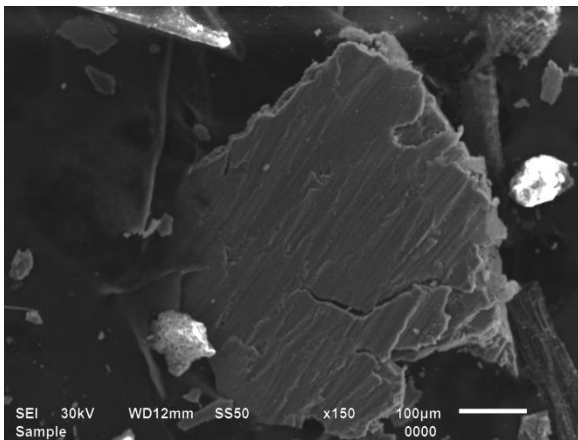
Wear debris of DPS 2 are presented in Fig. 18. The flake like morphology is observed at 1 kg load is similar to other composites debris. Zircon sand particle are also there in debris, which are debonded from the alloy matrix as shown in Fig. 18 (a-b). The debris generated having flake type morphology with microcracks resulted from the crack growth also the edge of flakes is not smooth. A long flake with embedded zircon sand particles is observed, which is pull out from the alloy matrix by excessive plastic deformation as shown in Fig. 18 (b). Coarse particle of zircon sand showing debonding at low loads itself and thus decreasing the wear resistance of the composite. At 2 kg load as shown in Fig. 18 (c) reveals the micro level delamination on a flake itself, which occur due number of microcracks. The long flakes with microcracks and flakes with embedded zircon sand particle is observed in wear debris generated at 3 kg load as shown in Fig. 18 (d). Flakes with embedded zircon sand particle can be attributed to the fact that coarse zircon sand particle are providing preferential crack and void nucleation site in the alloy matrix containing majority of fine particles. The deformation also is not homogeneous due to the presence of coarse particles in fine particle reinforced alloy matrix. At 4 kg load, the wear debris at higher load having flakes along with fragmented flakes as shown in Fig. 18(e). On higher load i.e. at 5 kg flakes showing extensive microcracks and small thin debris are there showing microcutting behavior as shown in Fig. 18 (f).



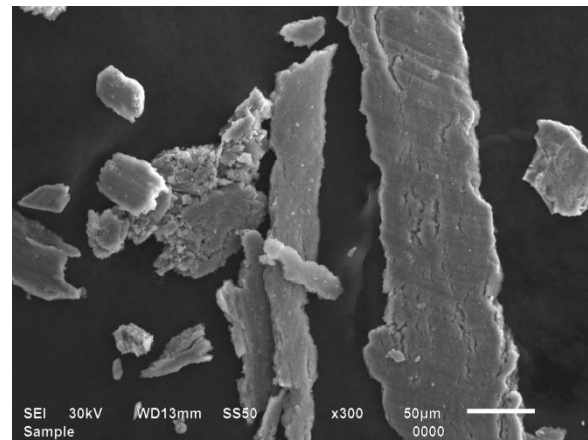
(a)



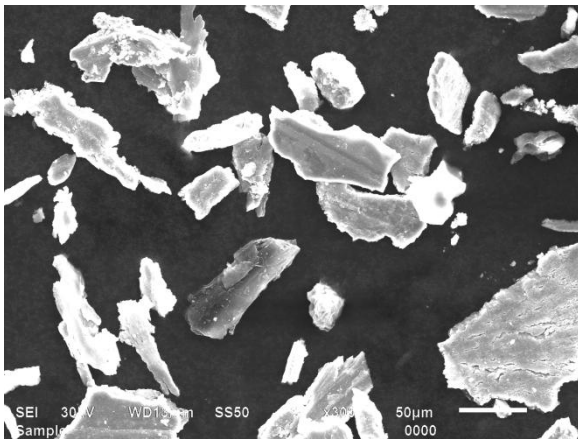
(b)



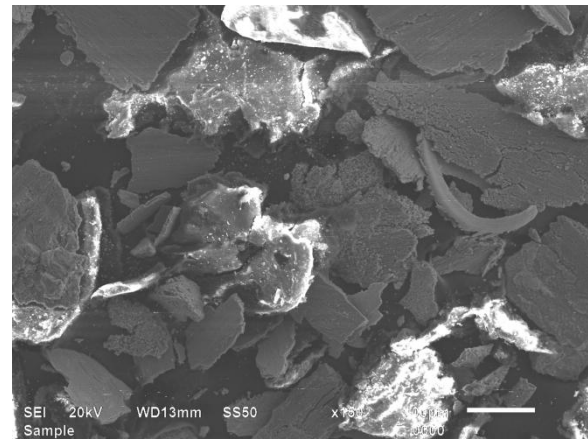
(c)



(d)



(e)



(f)

Fig.18. SEM micrograph of Wear debris generated of DPS 2 at (a) 1kg (b) 1kg (c) 2kg (d) 3kg (e) 4kg (f) 5kg

4.5 EDS Analysis

Wear debris EDS analysis is shown in Fig. 19, the EDS results indicate presence of Fe on wear debris which corresponds to the transfer of material from the counterpart disc to composite material. This also indicates that debris is generated by the rupture of mechanically mixed layer.

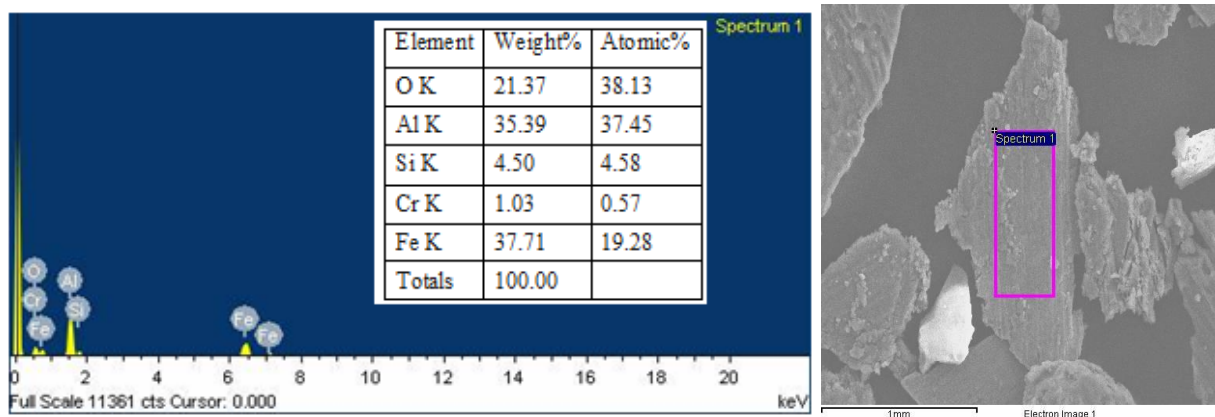


Fig.19. EDS analysis of wear debris

References cited in this chapter:

1. J. Hashim, L. Looney, M.S.J. Hashmi: Particle distribution in cast metal matrix composites—Part I. *Journal of Materials Processing Technology* 123 (2002) 251–257
2. J. Hashim, L. Looney, M.S.J. Hashmi: Particle distribution in cast metal matrix composites-Part II. *Journal of Materials Processing Technology* 12 (2002) 258–263
3. Y.M. Youssef, R.J. Dashwood, P. D. Lee: Effect of clustering on particle pushing and solidification behavior in TiB₂ reinforced aluminium PMMCs. *Composites: Part A* 36 (2005) 747–763
4. Hideo Nakae, Shusen Wu: Engulfment of Al₂O₃ particles during solidification of aluminum matrix composites. *Materials Science and Engineering A* 252 (1998) 232–238
5. J. Segurado, C. González, J. LLorca: A numerical investigation of the effect of particle clustering on the mechanical properties of composites. *Acta Materialia* 51 (2003) 2355–2369
6. Kleber S. Cruz, Elisangela S. Meza, Frederico A.P. Fernandes, Jose M.V. Quaresma, Luiz C. Casteletti, Amauri Garcia: Dendritic Arm Spacing Affecting Mechanical Properties and Wear Behavior of Al-Sn and Al-Si Alloys Directionally Solidified under Unsteady-State Conditions. *Metallurgical and Materials Transactions A*, Volume 41 A, April 2010—973
7. K. Kaur, O. P. Pandey: Wear and microstructural characteristics of spray atomized zircon sand reinforced LM13 alloy. *Mat.-wiss. u.Werkstofftech.* 2010, 41, No. 7
8. R. Singha Roy, H. Guchhait, A. Chanda, D. Basu, M. K. Mitra: Improved sliding wear-resistance of alumina with submicron grain size: A comparison with coarser grained material. *Journal of the European Ceramic Society* 27 (2007) 4737–4743
9. Sanjeev Das, V. Udhayabanu, S. Das, K. Das: Synthesis and characterization of zircon sand/Al-4.5 wt% Cu composite produced by stir casting route. *J. Mater Sci.* (2006) 41:4668–4677
10. S. K. Chaudhury, A. K. Singh, C. S. Sivaramakrishnan, S. C. Panigrahi: Wear and friction behavior of spray formed and stir cast Al–2Mg–11TiO₂ composites. *Wear* 258 (2005) 759–767
11. J. Zhang, A.T. Alpas: Transition between mild and severe wear in aluminium alloys. *Acta mater.* Vol. 45, No. 2, pp. 513-528, 1997

12. S.C. Sharma, B.M. Girish, D.R. Somashekar, B.M. Satish, Rathnakar Kamath: Sliding wear behaviour of zircon particles reinforced ZA-27 alloy composite materials. *Wear* 224 (1999) 89–94
13. Srinivasa R. Bakshi, Di Wang, Timothy Price, Deen Zhang, Anup K. Keshri, Yao Chen, D. Graham McCartney, Philip H. Shipway and Arvind Agarwal: Microstructure and wear properties of aluminum/aluminum-silicon composite coatings prepared by cold spraying. *Surface & Coatings Technology* 204 (2009) 503–51

CHAPTER 5

Conclusion and Future scope

5.1 Conclusion:

The present study is carried out to determine the influence of dual particle size zircon sand reinforcement on wear behavior of stir cast Al-Si alloy LM13. The wear study was carried out at five different loads at constant sliding distance and speed.

1. Zircon sand particle provides nucleation site for silicon during solidification, it is well confirmed by microstructure, EDS and line profile analysis.
2. Fine size zircon sand particle reinforced composite exhibits better wear resistance than coarse particle at same weight percentage of reinforcement.
3. Limited amount of fine particle size addition to coarse particle enhances the wear resistance as compared to single size coarse particle at same weight percentage of reinforcement.
4. Coarse particle addition to fine particle reinforced composite adversely affects the wear properties of the composite as compared to single size fine particle composite.

5.2 Future work of the study:

Different concentration of reinforcement should also be studied for further study. Further study about effect of temperature on wear behavior of composite may also be helpful to get idea about the reliability of the composite at higher temperature. Since the heat treated samples with different quenching media are showing good wear resistant properties, the work can be further extended to other quenching media like brine solution, oil quenching etc. The heat treatment temperatures of 400°C to 450°C are showing better wear resistance values. Therefore, at these temperatures the soaking time can be increased and further the wear properties can be evaluated.